Numerical investigation of shock instabilities in monatomic gases with extensions

Michael KAPPER[1], Jean-Luc CAMBIER[2]

[1] Austrian Space Research Institute, Graz, Austria

[2] Air Force Research Laboratory, Edwards AFB, CA, USA

Advanced Modeling & Simulation (AMS) Seminar Series

3 November 2016, NASA Ames

Outline

1. Governing equations
2. Numerical Formulation
3. Benchmarks
4. Collisional-Radiative Model
5. UTIAS Shocktube Experiments
6. Extensions & ongoing research
7. Moment equations
8. Conclusions

Personal background

- B.S., Organic Chemistry, U.C. Berkeley
- M.S., Mechanical Engineering, San Jose State
  - Prof. Periklis Papadopolous
  - Dr. Jean-Luc Cambier
- Ph.D., Mechanical Engineering, Ohio State
  - Dr. Jean-Luc Cambier
  - Prof. John Yu
- Postdoc, von Karman Institute for Fluid Dynamics
  - Prof. Thierry Magin
- Postdoc, Austrian Space Research Institute
  - Antenna Calibration, Solar Orbiter, JUICE
  - No in-house CFD

GOTchA

Goal

> Advanced Modeling & Simulation (M&S) of high-enthalpy plasma for propulsion, diagnostics, ...

Objectives

> Investigate new mathematical models & algorithms
> Develop advanced in-house M&S capability
> Validate physical models and numerical methods

Technical challenges

> Complexity of physical interactions
> Complexity of numerical approach

Approach

> Hybridize PIC and Fluid
> Multiple non-equilibrium descriptions (1T, 2T, CR, multifluid, non-Maxwellian, ...)
> Object-Oriented programming / Multi-threading / Java

GOTchA

Goal

> Advanced Modeling & Simulation (M&S) of high-enthalpy plasma for propulsion, diagnostics, ...

Objectives

> Investigate new mathematical models & algorithms
> Develop advanced in-house M&S capability
> Validate physical models and numerical methods

Technical challenges

> Complexity of physical interactions
> Complexity of numerical approach

Approach

> Hybridize PIC and Fluid
> Multiple non-equilibrium descriptions (1T, 2T, CR, multifluid, non-Maxwellian, ...)
> Object-Oriented programming / Multi-threading / Java

GOTchA

Goal

> Advanced Modeling & Simulation (M&S) of high-enthalpy plasma for propulsion, diagnostics, ...

Objectives

> Investigate new mathematical models & algorithms
> Develop advanced in-house M&S capability
> Validate physical models and numerical methods

Technical challenges

> Complexity of physical interactions
> Complexity of numerical approach

Approach

> Hybridize PIC and Fluid
> Multiple non-equilibrium descriptions (1T, 2T, CR, multifluid, non-Maxwellian, ...)
> Object-Oriented programming / Multi-threading / Java

GOTchA

Goal

> Advanced Modeling & Simulation (M&S) of high-enthalpy plasma for propulsion, diagnostics, ...

Objectives

> Investigate new mathematical models & algorithms
> Develop advanced in-house M&S capability
> Validate physical models and numerical methods

Technical challenges

> Complexity of physical interactions
> Complexity of numerical approach

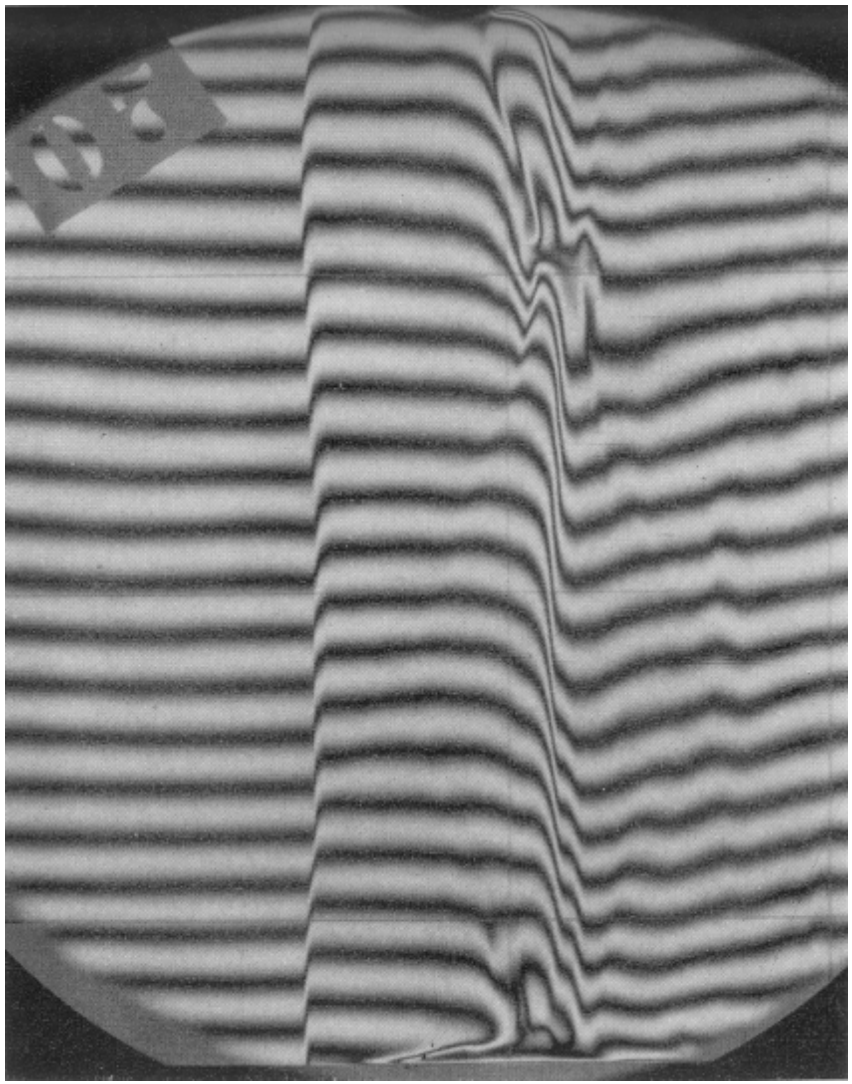
Approach

> Hybridize PIC and Fluid
> Multiple non-equilibrium descriptions (1T, 2T, CR, multifluid, non-Maxwellian, ...)
> Object-Oriented programming / Multi-threading / Java

Case in Point: Strong Ionizing Shock in Argon

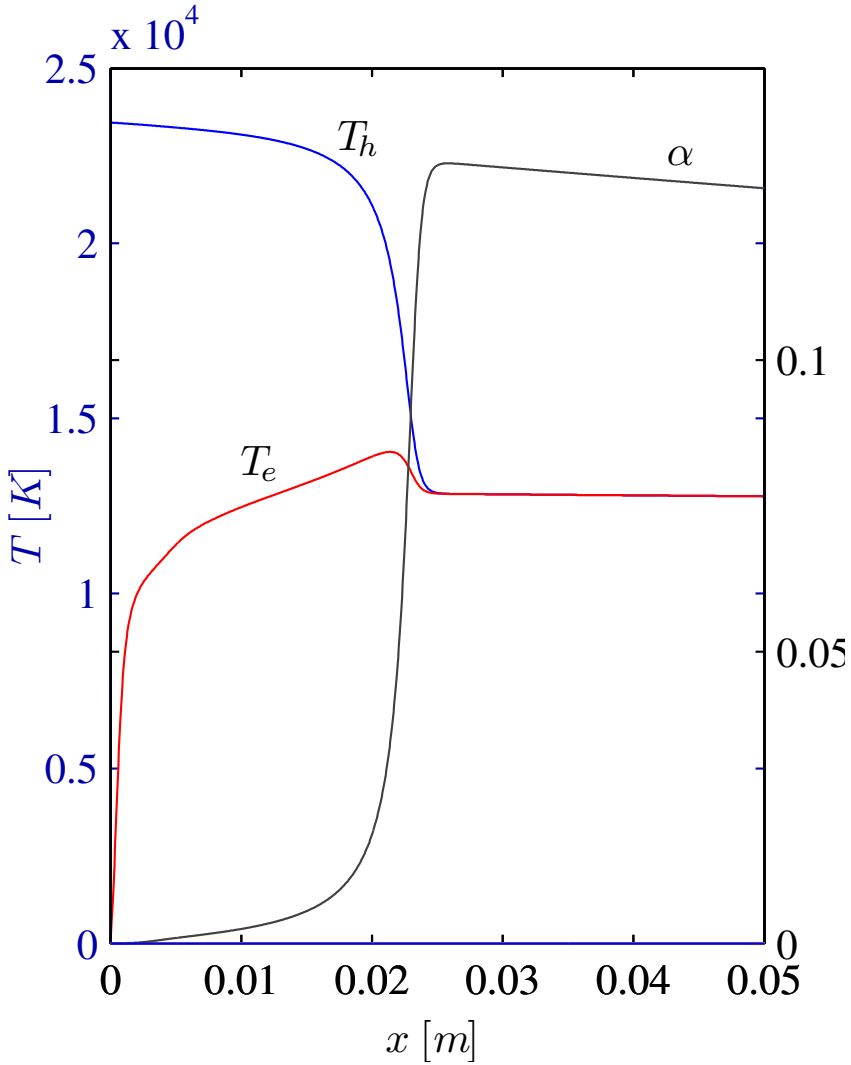
- Shock tubes have been invaluable in research of non-equilibrium kinetics
- A very unique and interesting series of shock tube experiments conducted at UTIAS indicate a strong coupling between unsteady shock phenomena and ionization kinetics
- The translational shock front propagating in pure Argon "develops sinusoidal instabilites which affect the entire shock structure including the relaxation region, the electron cascade front, and the final quasi-equilibrium state"
- Similarities noted between detonation waves

Glass & Liu (UTIAS)



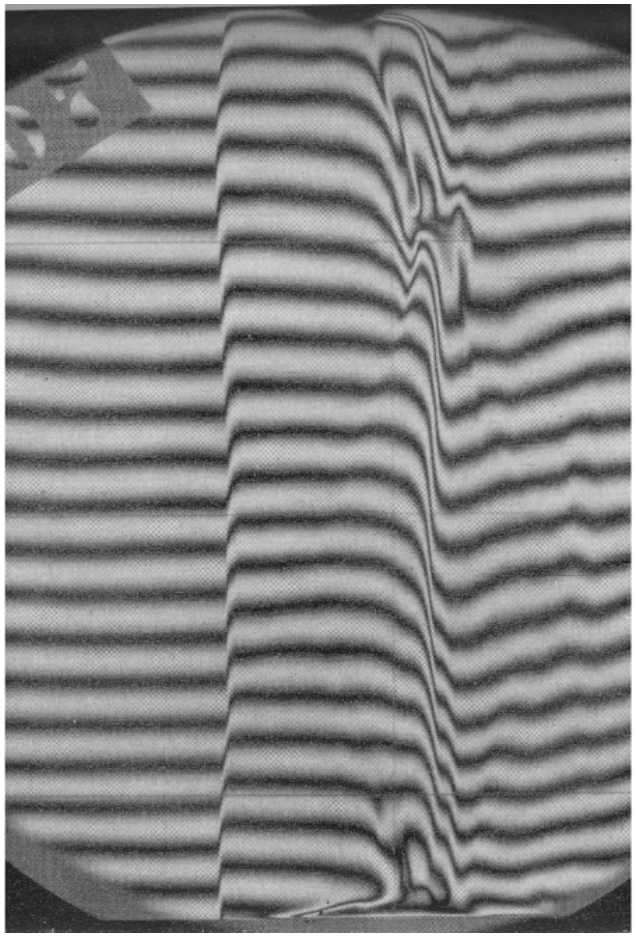
Details of shock structure

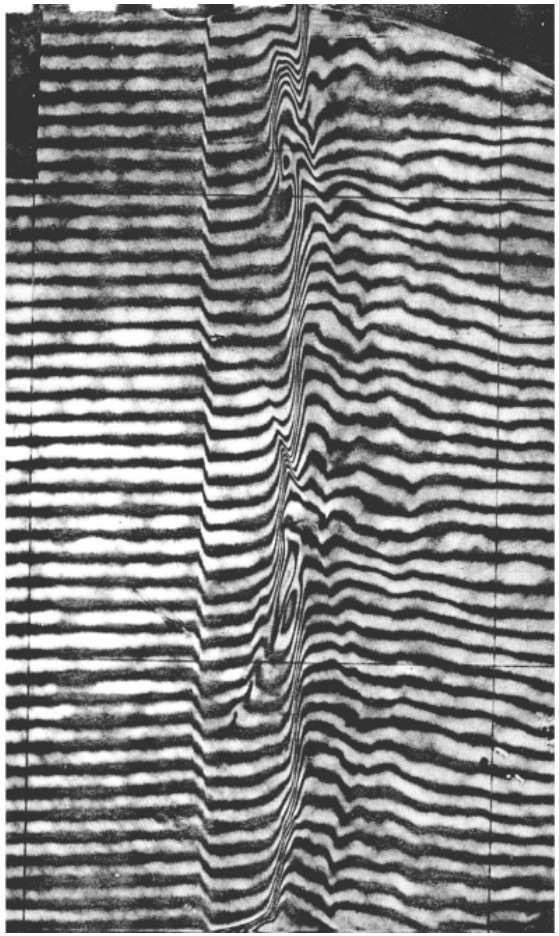
- First detailed study by Petschek & Byron, 1957
- Slowest time scale is that of ionization equilibrium which consequently determines relaxation length
- Kinetics must be time resolved in order to resolve shock stucture ← non-equilibrium!

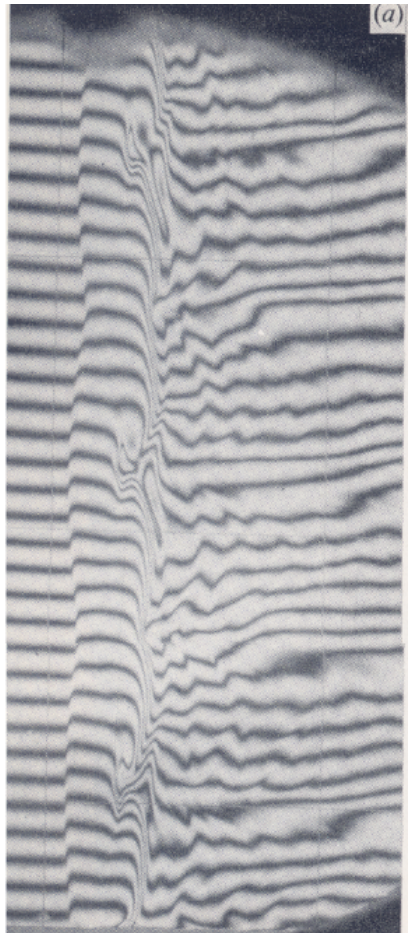


Effect of Mach number

Ma = 14.7, 16.1, 17.0







Objective: Modeling Dynamic Effects

- Initial work on simulating the unsteady nature of ionizing shocks indicated a coupling between gasdynamics and ionization kinetics through pressure waves (Cambier 1991)
- High sensitivity of kinetics to small perturbations in the local temperature
- Similar mechanism to that found in detonation waves
- Do similarities extend to multiple dimensions?

GOAL: Develop detailed kinetic model (CR) for argon and couple with high-order transport solver to reproduce dynamic instabilities

Outline

1 Governing equations
2 Numerical Formulation
3 Benchmarks
4 Collisional-Radiative Model
5 UTIAS Shocktube Experiments
6 Extensions & ongoing research
7 Moment equations
8 Conclusions

Governing Equations

mass:

$$\frac{\partial \rho_s}{\partial t} + \nabla \cdot (\rho_s \vec{u}_s) = \dot{\rho}_s \tag{1}$$

momentum:

$$\frac{\partial \rho_s \vec{u}_s}{\partial t} + \nabla \cdot (\rho_s \vec{u}_s \vec{u}_s) + \nabla p_s = \vec{\mu}_s + n_s e Z_s (\vec{E} + \vec{u}_s \times \vec{B}) \tag{2}$$

energy:

$$\frac{\partial \rho_s \varepsilon_s}{\partial t} + \nabla \cdot (\vec{u}_s (\rho_s \varepsilon_s + p_s)) = \vec{u}_s \cdot \vec{\mu}_s - n_s e Z_s \vec{u}_s \cdot \vec{E} - \nabla \cdot (\bar{\bar{\kappa}}_s \nabla T_s) - \dot{q}_s^{\text{cr}} \tag{3}$$

- Plasma is collision-dominated $\rightarrow$ fluid description
- Characteristic length scales larger than Debye length: electrons are rigidly coupled to ions, $\vec{u}_i \approx \vec{u}_n \approx \vec{u}_e \approx \vec{u}$
- Maxwellian distribution of atoms and electrons is extremely fast
- $T_i \approx T_n$ since their similar masses lead to rapid thermalization
- However, $T_e \neq T_a$ due to disparate masses resulting in slow thermalization
- Very high electron mobility $\rightarrow$ electron heat conduction greatly exceeds that for ions

Governing Equations: Two-Fluid Description

mass:

$$\frac{\partial \rho_i}{\partial t} + \nabla \cdot (\rho_i \vec{u}) = \dot{\rho}_i \tag{4}$$

$$\frac{\partial \rho_e}{\partial t} + \nabla \cdot (\rho_e \vec{u}) = \dot{\rho}_e \tag{5}$$

momentum:

$$\frac{\partial \rho_i \vec{u}}{\partial t} + \nabla \cdot (\rho_i \vec{u}\vec{u}) + \nabla p_i = n_i e Z_i (\vec{E} + \cancelto{0}{\vec{u} \times \vec{B}}) \tag{6}$$

$$\cancelto{0}{\frac{\partial \rho_e \vec{u}}{\partial t}} + \cancelto{0}{\nabla \cdot (\rho_e \vec{u}\vec{u})} + \nabla p_e = n_e e Z_e (\vec{E} + \cancelto{0}{\vec{u} \times \vec{B}}) \tag{7}$$

energy:

$$\frac{\partial \rho_i \varepsilon_i}{\partial t} + \nabla \cdot (\vec{u}(\rho_i \varepsilon_i + p_i)) = -n_i e Z_i \vec{u} \cdot \vec{E} - \dot{q}_i \tag{8}$$

$$\frac{\partial \rho_e \varepsilon_e}{\partial t} + \nabla \cdot (\vec{u}(\rho_e \varepsilon_e + p_e)) = -n_e e Z_e \vec{u} \cdot \vec{E} - \dot{q}_e \tag{9}$$

Reduce to 1-Fluid, 2-Temperature

mass:

$$\frac{\partial \rho}{\partial t} + \nabla \cdot (\rho \vec{u}) = \dot{\rho} \tag{10}$$

(11)

momentum:

$$\frac{\partial \rho \vec{u}}{\partial t} + \nabla \cdot (\rho \vec{u} \vec{u}) + \nabla (p_i + p_e) = 0 \tag{12}$$

(13)

energy:

$$\frac{\partial \rho \varepsilon}{\partial t} + \nabla \cdot (\vec{u}(\rho \varepsilon + p_i + p_e)) = -\dot{q}_i \tag{14}$$

$$\frac{\partial \rho_e \varepsilon_e}{\partial t} + \nabla \cdot (\rho_e \varepsilon_e \vec{u}) = -p_e \nabla \cdot \vec{u} - \dot{q}_e \tag{15}$$

Electron entropy formulation

The term $p_e \nabla \cdot \vec{u}$ is nonconservative and leads to errors in jump conditions across shock. This term can be eliminated by reformulating in terms of entropy:

$$\frac{\partial \rho \hat{s}_e}{\partial t} + \nabla \cdot (\rho \hat{s}_e \vec{u}) = -\frac{\gamma_e - 1}{\rho^{\gamma_e - 1}} \dot{q}_e \tag{16}$$

This is justifiable! The ion temperature jump across the shock is of the order $\Delta T_i \sim m_i V^2/k$, while for electrons it is $\Delta T_e \sim m_e V^2/k$. The electrons are heated adiabatically: The electrons are rigidly bound to the ions via electric forces and are compressed in the same manner. Dissipation of energy due to electron viscous forces is negligibly small (Zel′dovich & Raizer).

Summary of the Governing Equations

- Integral form of the governing equations

$$\frac{d}{dt}\int_{V(t)} Q\ dV + \oint_{A(t)} \hat{n}\cdot\bar{\bar{F}}\ dA = \int_{V(t)} \dot{\Omega}\ dV \tag{17}$$

- with conservative variable and flux vectors

$$Q = \begin{pmatrix} \rho_1 \\ \vdots \\ \rho_N \\ \rho u \\ \rho v \\ \rho w \\ E \\ \rho \hat{s}_e \end{pmatrix}, \quad F_n = \begin{pmatrix} \rho_1 v_n \\ \vdots \\ \rho_N v_n \\ \rho u v_n + n_x p \\ \rho v v_n + n_y p \\ \rho w v_n + n_z p \\ H_\circ v_n \\ \rho \hat{s}_e v_n \end{pmatrix} \tag{18}$$

$$E = E_h + E_e + \frac{1}{2}\rho\vec{u}\cdot\vec{u}, \quad H_\circ = E + p, \quad \hat{s}_e = \frac{p_e}{\rho^{\gamma_e}} \tag{19}$$

Equation of State—Ideal Gas

Dalton's Law:

$$p = p_h + p_e, \tag{20}$$

Total Energy:

$$E = \sum_{s \neq e} \rho_s \varepsilon_s + \rho_e \varepsilon_e + \frac{\vec{m} \cdot \vec{m}}{2\rho} + \frac{\vec{B} \cdot \vec{B}}{2\mu_\circ} \tag{21}$$

Heavy-particle fluid (thermally-perfect)

Thermal EOS: $$p_h = T_h \sum_{s \neq e} \rho_s R_s \tag{22}$$

Caloric EOS: $$d\varepsilon_s = c_{v,s}\, dT_h \tag{23}$$

Electron fluid (calorically-perfect, isentropic)

Isentropic flow: $$p_e = S_e \rho^{\gamma_e - 1} \tag{24}$$

Caloric EOS: $$\varepsilon_e = \frac{p_e}{\rho_e(\gamma_e - 1)} \tag{25}$$

$$dp = (\gamma_h - 1)\left[dE + \frac{1}{2}\vec{u}\cdot\vec{u}d\rho - \vec{u}\cdot d\vec{m} - \frac{1}{\mu_\circ}\vec{B}\cdot d\vec{B} - \sum_{s\neq e}\varepsilon_s d\rho_s - \frac{\rho^{\gamma_e-1}}{\gamma_e - 1}dS_e\right] + T_h \sum_{s\neq e} R_s d\rho_s + \rho^{\gamma_e - 1} dS_e + (\gamma_e - \gamma_h)\frac{p_e}{\rho}d\rho \tag{26}$$

$$\gamma_h - 1 \equiv \frac{\sum_{s\neq e}\rho_s R_s}{\sum_{s\neq e}\rho_s c_{v,s}} \tag{27}$$

$$dE = \frac{1}{\gamma_h - 1}\left[dp - T_h \sum_{s\neq e} R_s d\rho_s - dp_e\right] + \sum_{s\neq e}\varepsilon_s d\rho_s + \frac{dp_e}{\gamma_e - 1} + \rho\vec{u}\cdot d\vec{u} + \frac{1}{2}\vec{u}\cdot\vec{u}d\rho + \frac{1}{\mu_\circ}\vec{B}\cdot d\vec{B}, \tag{28}$$

Outline

1. Governing equations
2. Numerical Formulation
3. Benchmarks
4. Collisional-Radiative Model
5. UTIAS Shocktube Experiments
6. Extensions & ongoing research
7. Moment equations
8. Conclusions

The Semi-Discrete Approach

- Start with a discretization for the spatial terms while leaving the time derivative unmodified: PDE's $\rightarrow$ ODE's
- Numerically integrate to advance solution in time, ODE's $\rightarrow$ OΔE's

Spatial discretization

$$\frac{dQ}{dt} + \frac{1}{V}\sum_s F_{n,s} A_s = S \tag{29}$$

The flux function can be approximated as

$$\hat{F}_s = \frac{1}{2}(F_L + F_R) - \Phi \tag{30}$$

Introducing an *upwind* bias,

$$\Phi = \frac{1}{2}|A_s|(Q_R - Q_L) \tag{31}$$

where

$$|A| \equiv R|\Lambda|L \tag{32}$$

At surface s, pure upwinding is achieved if

$$F_s = \begin{cases} F_L & \text{if } |\Lambda| = \Lambda \\ F_R & \text{if } |\Lambda| = -\Lambda \end{cases} \tag{33}$$

This condition can only be achieved if A_s in Eq. (31) satisfies

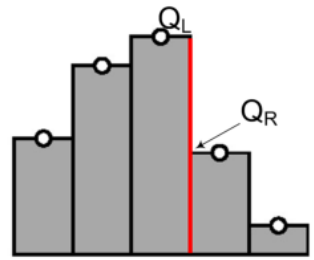
$$F_R - F_L = A_s(Q_R - Q_L) \tag{34}$$

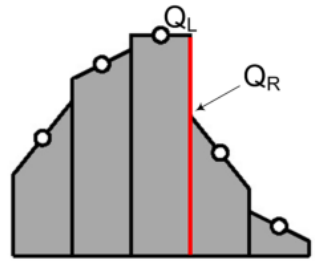
This defines the Roe-average values.

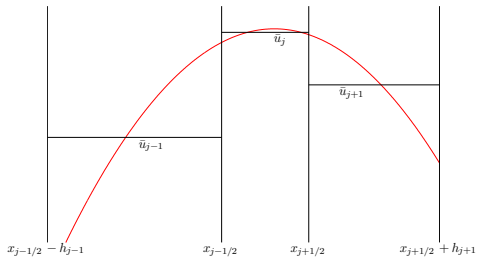
Reconstruction

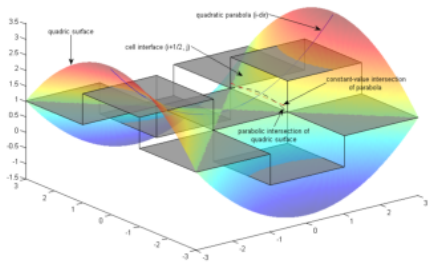
- The numerical flux function at a cell interface has been defined as $F_s = \frac{1}{2}(F_L + F_R) - \Phi$
- How are F_L and F_R chosen?
  - Use cell-average information from left and right cells $\rightarrow$ very diffusive, yet stable
  - Use information from multiple cells (stencil) $\rightarrow$ delicate balance between accuracy and stability

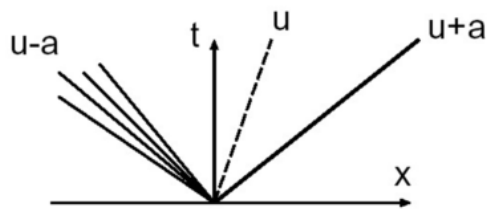
Reconstruction procedure











$$Q_L = \frac{1}{6}(2\bar{Q}_{j-1} + 5\bar{Q}_j - \bar{Q}_{j+1})$$

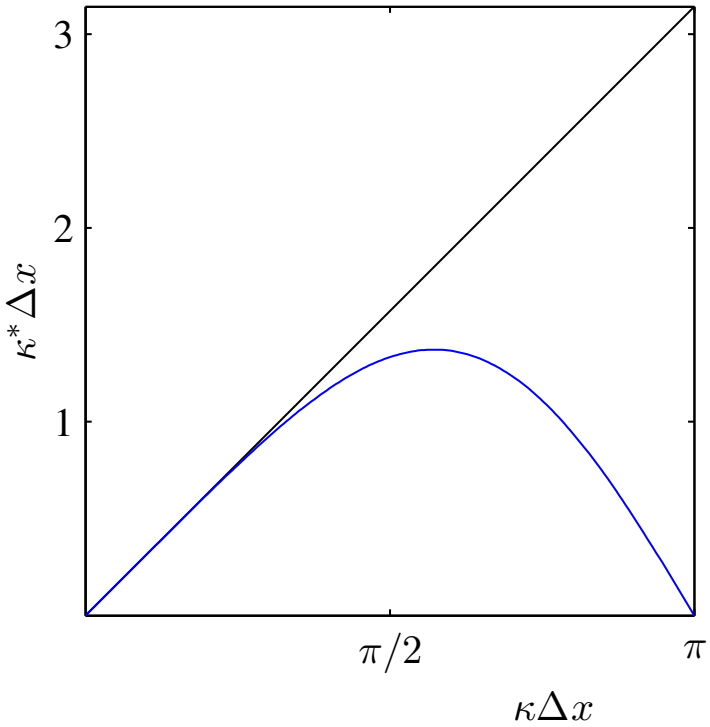
$$Q_L \leftarrow \text{median}(Q_L,\ \bar{Q}_j,\ Q^{MP})$$

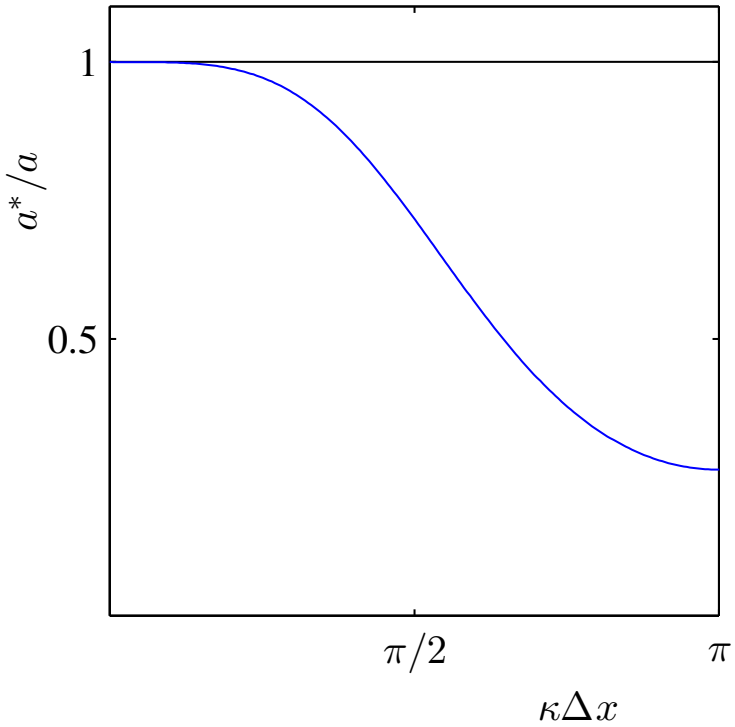
$$Q^{MP} = \bar{Q}_j + \text{minmod}[\bar{Q}_{j+1} - \bar{Q}_j,\ \alpha(\bar{Q}_j - \bar{Q}_{j-1})]$$

Model linear advection

$$\frac{\partial u}{\partial t} + a\frac{\partial u}{\partial x} = 0, \tag{35}$$

$$\frac{d\vec{u}}{dt} = L\vec{u}, \quad L = \frac{a}{\Delta x}\frac{1}{6}B_p(M:-1,6,-3,-2,0) \tag{36}$$





Numerical Integration

$$\frac{du}{dt} = L(u^n) \tag{37}$$

$$\int_{t_n}^{t_{n+1}} \left(du = L(u^n) \right) dt \tag{38}$$

- Integrate in time to advance solution
- Method selection is not necessarily trivial!
  - accuracy, stability, efficiency

2nd-Order Runge-Kutta (Predictor-Corrector)

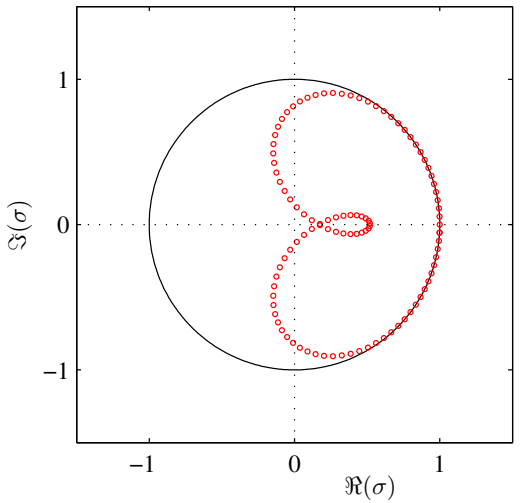
$$u^{n+1/2} = u^n + \Delta t L(u^n) \tag{39a}$$

$$u^{n+1} = u^n + \frac{1}{2}\Delta t L(u^n + u^{n+1/2}) \tag{39b}$$

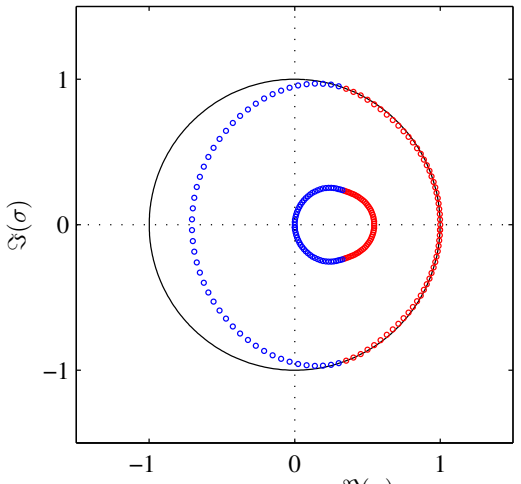
2nd-Order Adams-Bashforth (Multistep)

$$u^{n+1} = u^n + \frac{1}{2}\Delta t L(3u^n - u^{n-1}) \tag{40}$$

2nd-Order Runge-Kutta, CFL = 0.9



2nd-Order Adams-Bashforth, CFL = 0.58

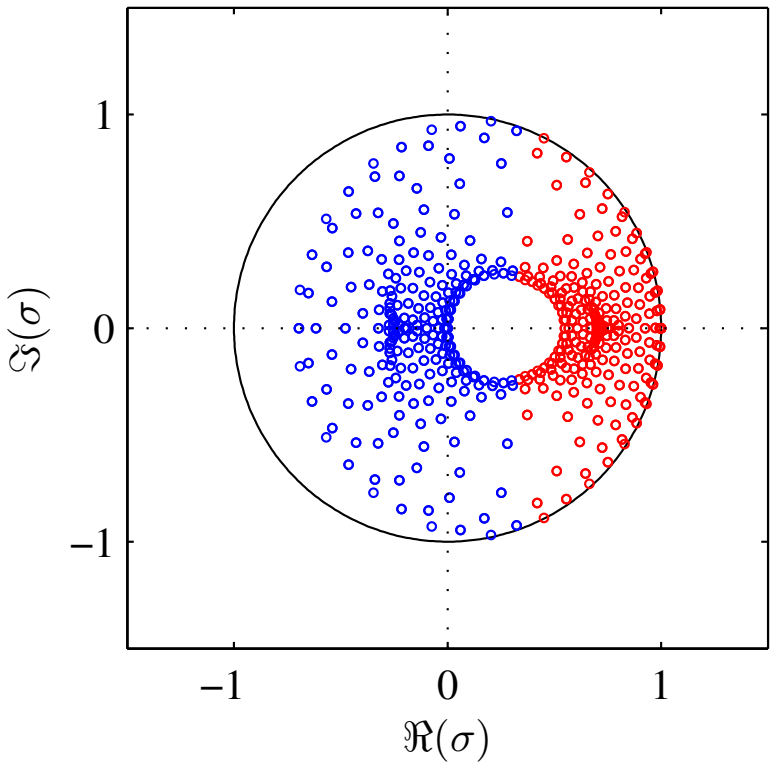


The λ-σ relation

$$\frac{d\vec{u}}{dt} = L\vec{u}, \quad u^{n+1} = Su^n \tag{41}$$

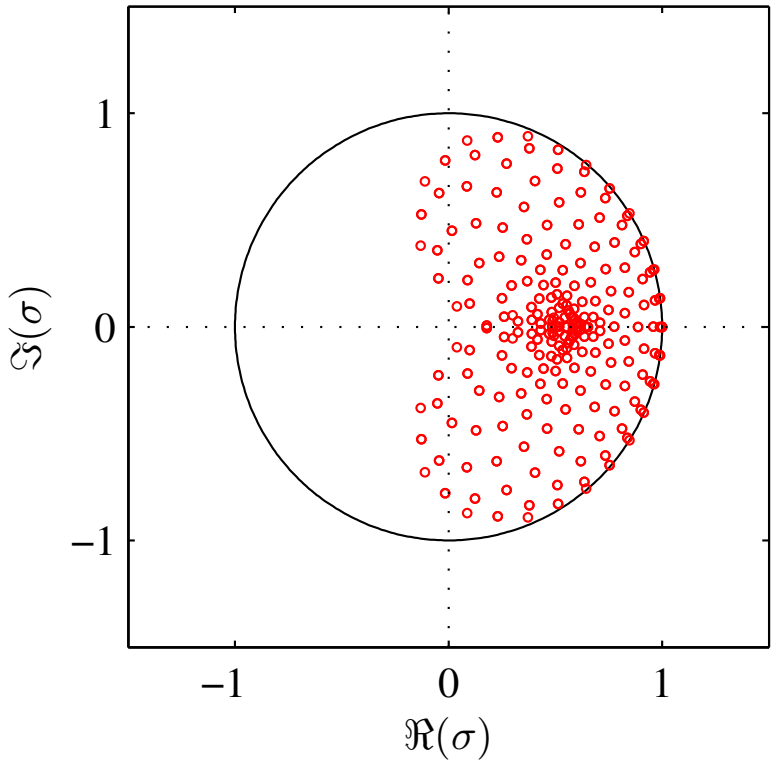
AB2 stable up to CFL$= 0.29$

$$\sigma^2 - \left(1 + \frac{3}{2}\lambda\Delta x\right)\sigma + \frac{1}{2}\lambda\Delta x = 0$$



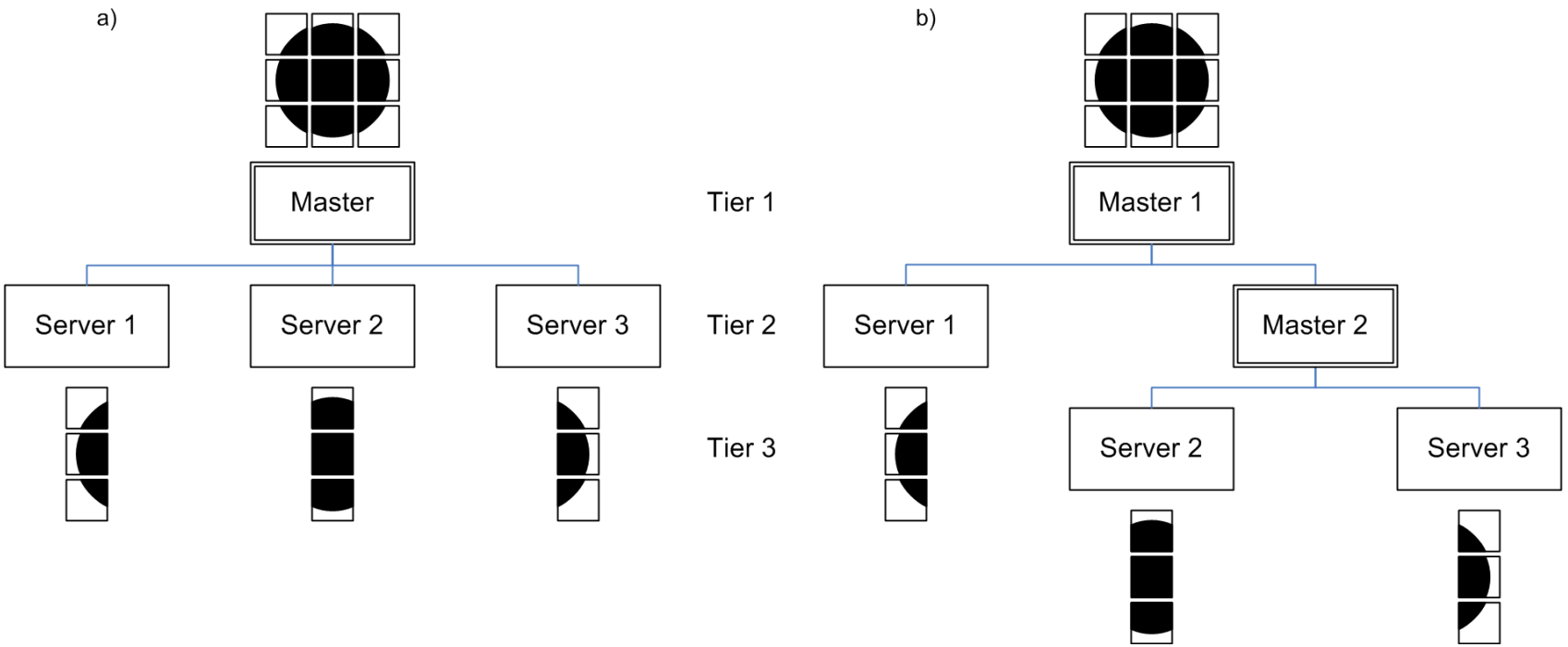
RK2 stable up to CFL$= 0.45$

$$\sigma - 1 - \lambda\Delta x - \frac{1}{2}\lambda^2\Delta x^2 = 0$$



Parallelization Framework: Java Remote Method Invocation (RMI)

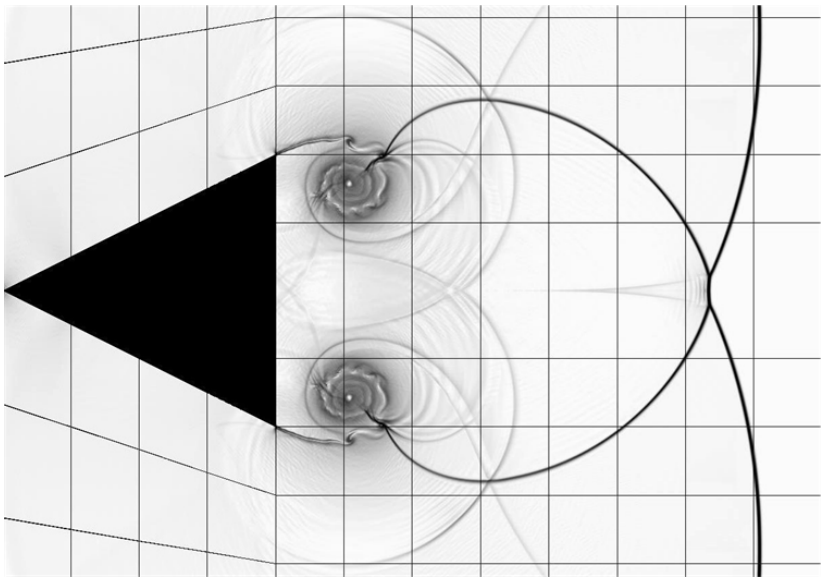
- Fully Object-Oriented, multi-threaded code
- Java Native Interface (JNI) for accessing C/C++/Fortran
- Shared- and distributed-memory hardware in tree configuration

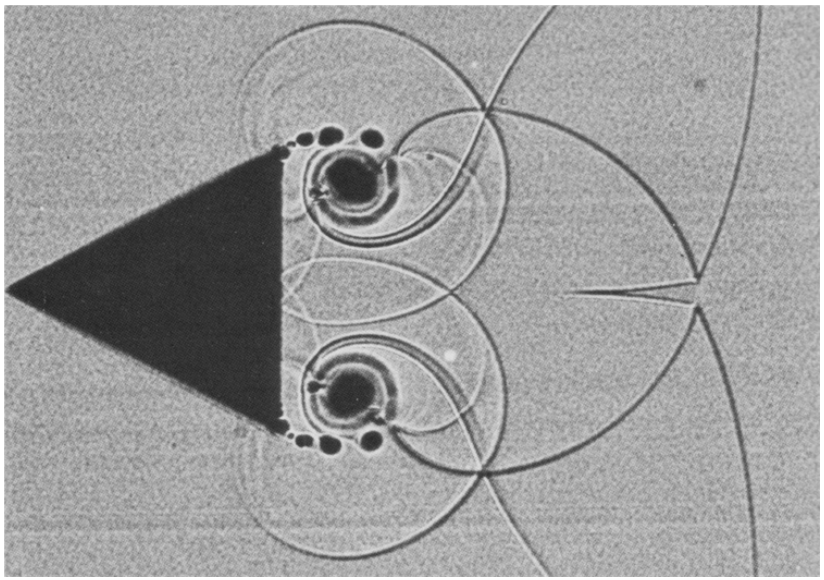


Outline

1. Governing equations
2. Numerical Formulation
3. Benchmarks
4. Collisional-Radiative Model
5. UTIAS Shocktube Experiments
6. Extensions & ongoing research
7. Moment equations
8. Conclusions

Schardin's problem: Mach 1.3 shock diffraction past wedge





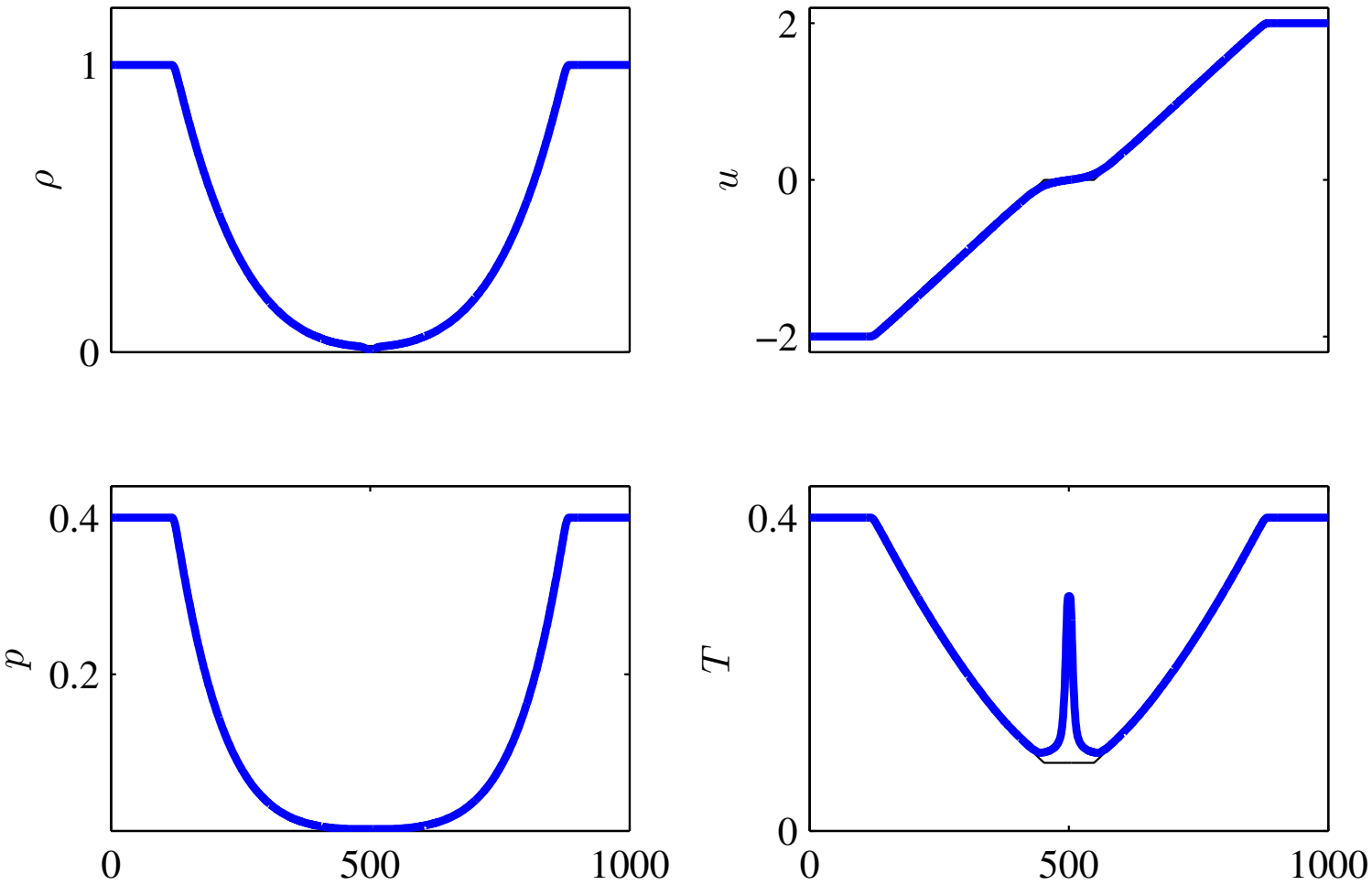
Mach 5.09 shock diffraction down step (Bazhenova et al.)

Emery Mach 3 wind tunnel

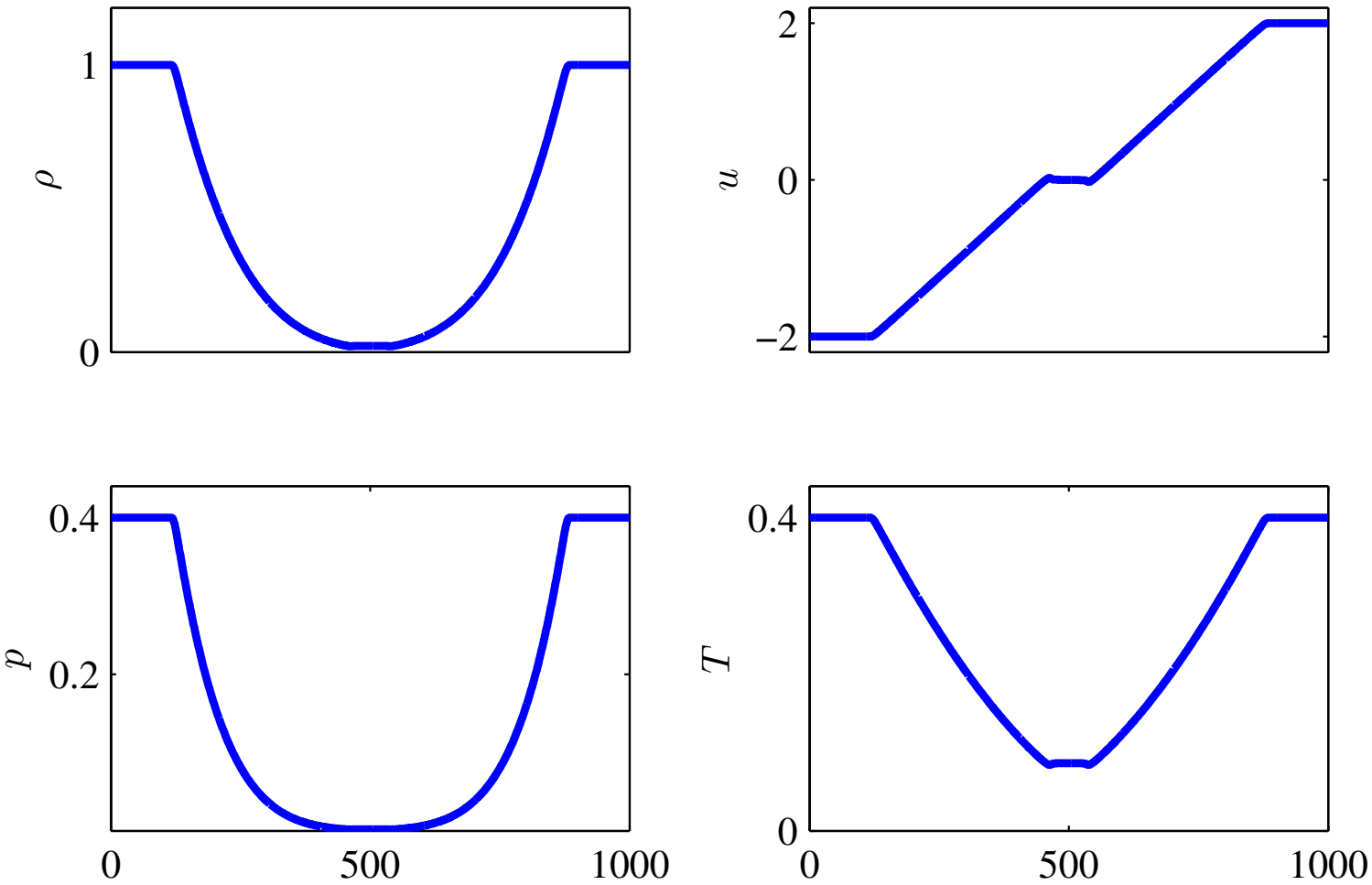
Rayleigh-Taylor instability

Orszag-Tang Ideal MHD vortex

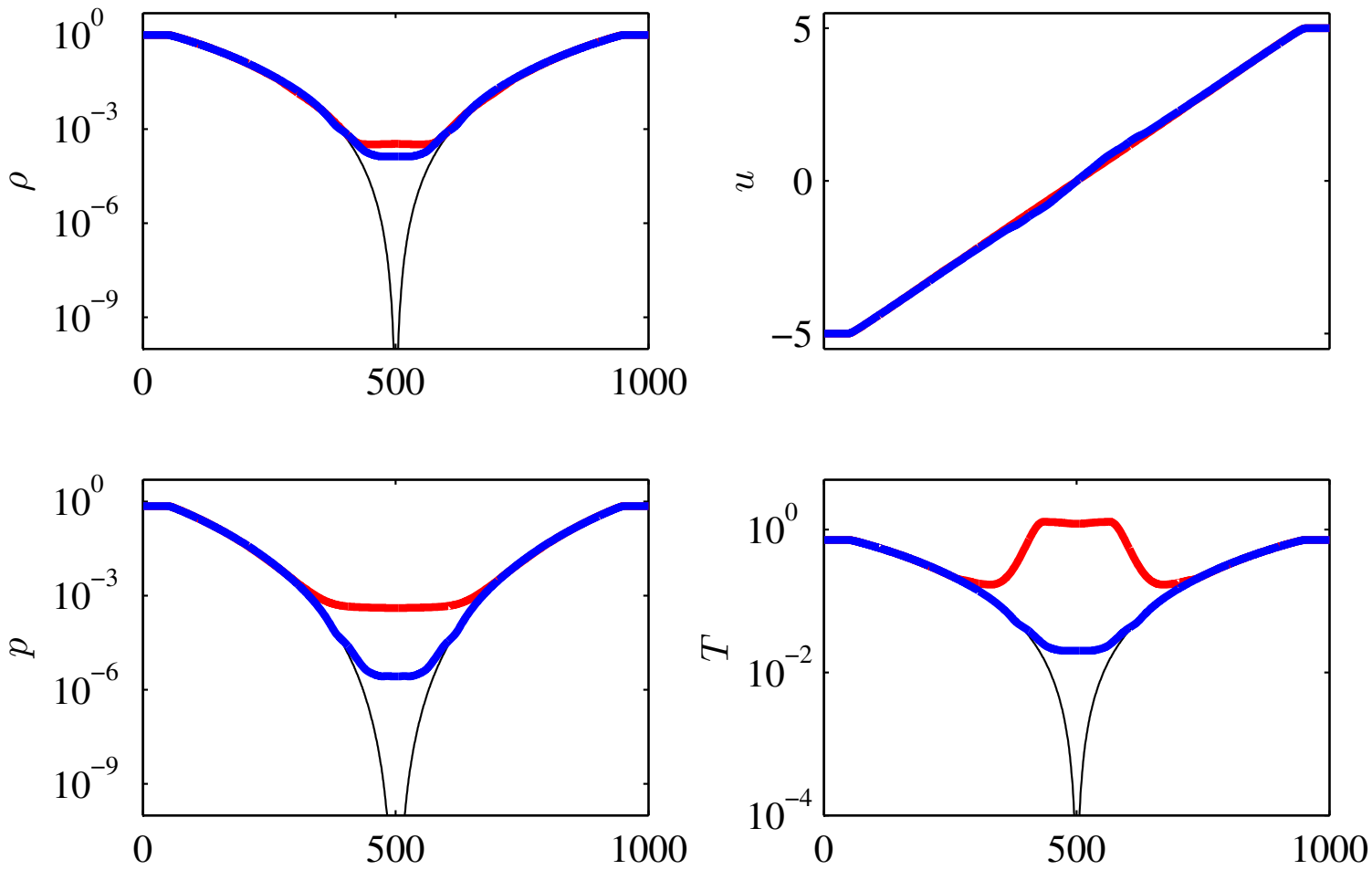
Einfeldt's 1-2-3 Strong Rarefaction: Energy Conservation



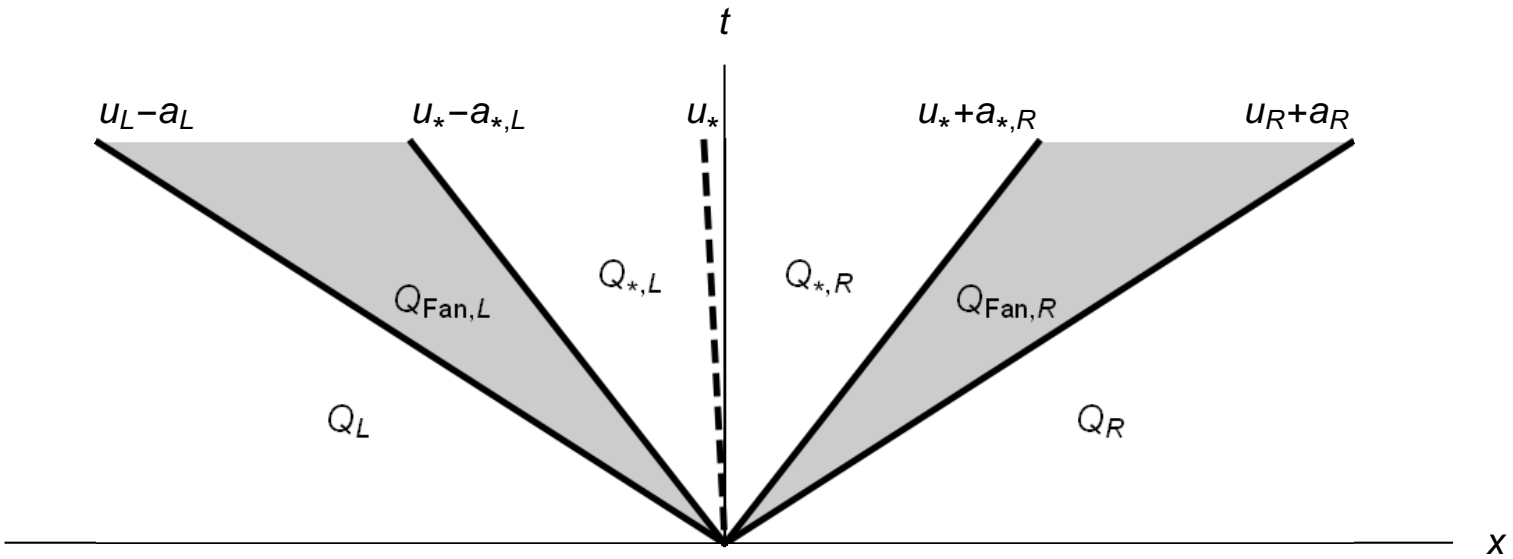
Einfeldt's 1-2-3 Strong Rarefaction: Entropy Conservation



Vacuum Test


ρ
10^0
10^{-3}
10^{-6}
10^{-9}
0
500
1000
u
5
0
−5
p
10^0
10^{-3}
10^{-6}
10^{-9}
0
500
1000
T
10^0
10^{-2}
10^{-4}
0
500
1000

Fan of characteristics for Riemann problem



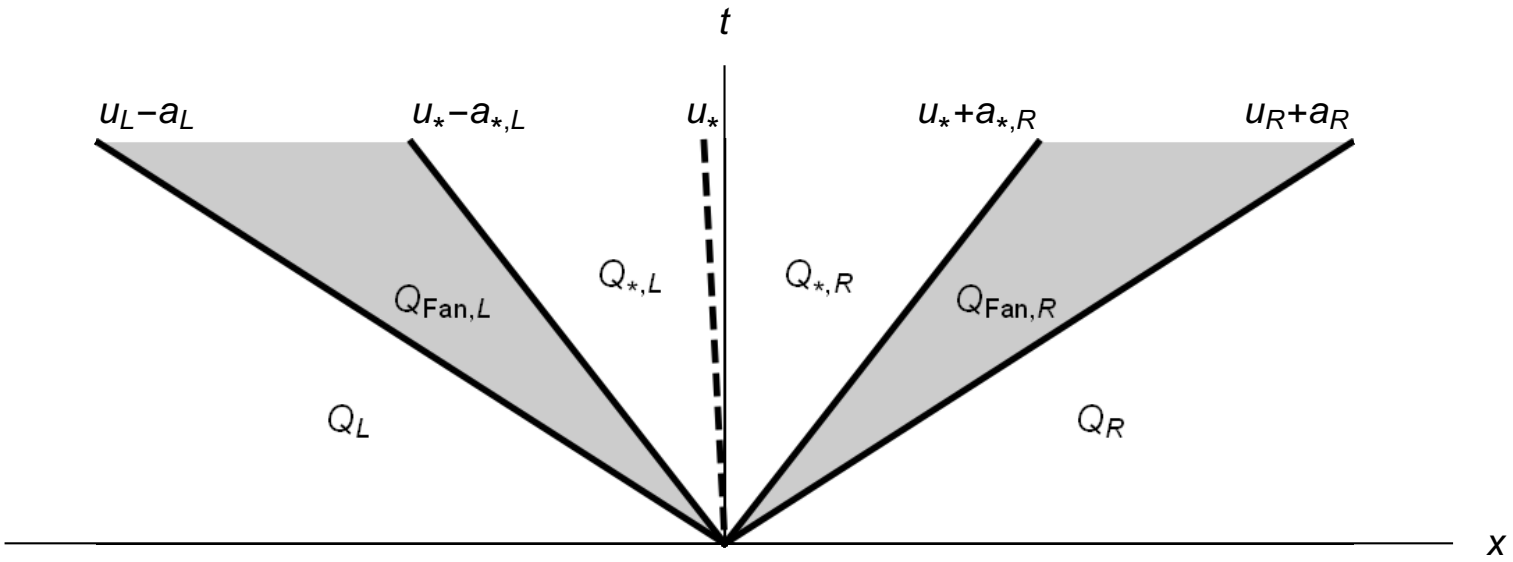
α^k are coefficients of the projection of ΔQ onto $\vec{r}$

$$Q_R - Q_L = \sum_{k=1}^{N} \alpha^k \vec{r}^k \tag{42}$$

jump across k-th wave

$$\Delta Q^k = \alpha^k \vec{r}^k \tag{43}$$

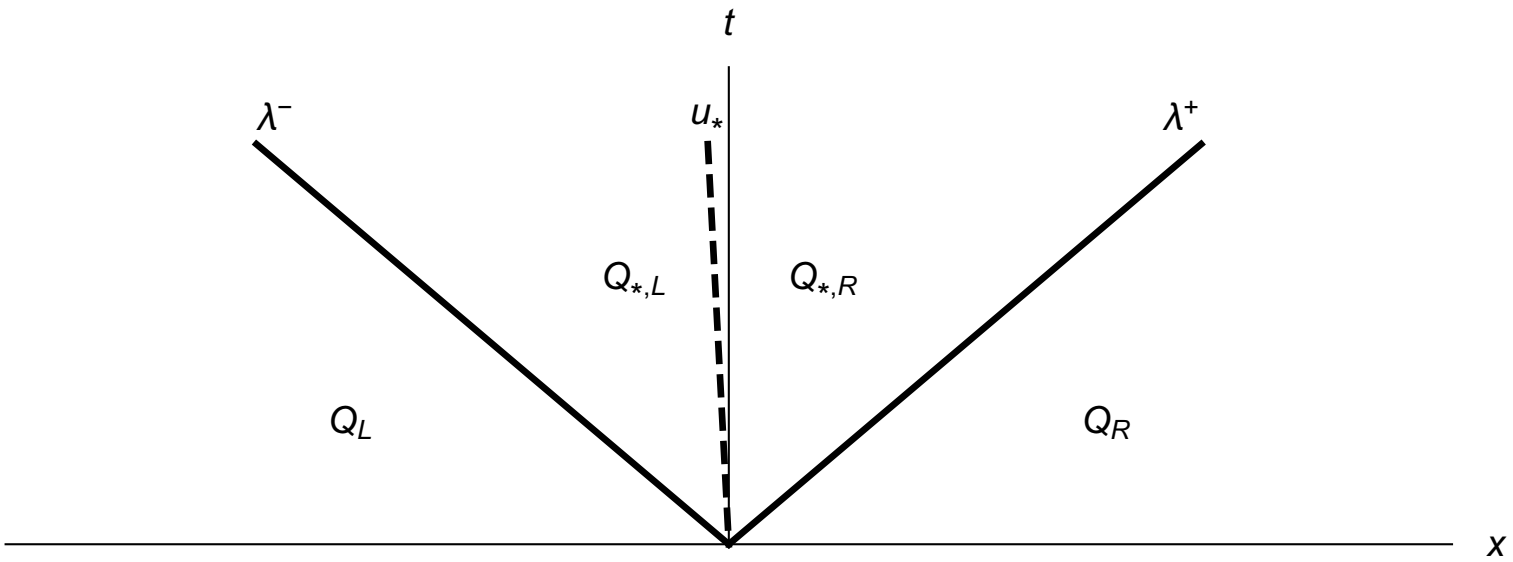
Fan of characteristics for Riemann problem



$$F^{\text{Roe}}_{i+1/2} = \frac{1}{2}\left\{ F_L + F_R - \sum_{k=1}^{N} |\lambda^k_{i+1/2}| \alpha^k_{i+1/2} \vec{r}^k_{i+1/2} \right\} \tag{44}$$

$$\sum_{k=1}^{N} |\lambda^k_{i+1/2}| \alpha^k_{i+1/2} \vec{r}^k_{i+1/2} = |u_L - a_L|(Q_{\text{Fan},L} - Q_L) + |u_* - a_{*,L}|(Q_{*,L} - Q_{\text{Fan},L})$$
$$+ |u_*|(Q_{*,R} - Q_{*,L}) + |u_* + a_{*,R}|(Q_{\text{Fan},R} - Q_{*,R}) + |u_R + a_R|(Q_R - Q_{\text{Fan},R}) \tag{45}$$

Fan of characteristics for Riemann problem



What are equivalent λ^- & λ^+?

$$\sum_{k=1}^{N} |\lambda_{i+1/2}^k| \alpha_{i+1/2}^k \vec{r}_{i+1/2}^k = |\lambda^-|(Q_{*,L} - Q_L) + |u_*|(Q_{*,R} - Q_{*,L}) + |\lambda^+|(Q_R - Q_{*,R}) \quad (46)$$

Isentropic system

$$\vec{r}_1 = \begin{pmatrix} 1 \\ \lambda^- \\ s \end{pmatrix}, \quad \vec{r}_2 = \begin{pmatrix} 1 \\ u \\ \frac{\partial S}{\partial \rho} \end{pmatrix}, \quad \vec{r}_3 = \begin{pmatrix} 1 \\ \lambda^+ \\ s \end{pmatrix} \tag{47}$$

Entropy conservation

$$Q = \begin{pmatrix} \rho \\ \rho u \\ S \end{pmatrix}, \quad F = \begin{pmatrix} \rho u \\ \rho u^2 + p \\ uS \end{pmatrix} \tag{48}$$

$$p = \rho^{\gamma - 1} S \tag{49}$$

Isentropic system

$$\vec{r}_1 = \begin{pmatrix} 1 \\ \lambda^- \\ s_L \end{pmatrix}, \quad \vec{r}_2 = \begin{pmatrix} 1 \\ u_* \\ \frac{\partial S}{\partial \rho} \end{pmatrix}, \quad \vec{r}_3 = \begin{pmatrix} 1 \\ \lambda^+ \\ s_R \end{pmatrix} \tag{50}$$

Ensure $p_{*,L} = p_{*,R}$ & $u_{*,L} = u_{*,R}$ across contact wave

$$u_* = \frac{p_R^{1/\gamma}(\lambda^+ - u_R)\lambda^- - p_L^{1/\gamma}(\lambda^- - u_L)\lambda^+}{p_R^{1/\gamma}(\lambda^+ - u_R) - p_L^{1/\gamma}(\lambda^- - u_L)} \tag{51}$$

$$\frac{\partial S}{\partial \rho} = \frac{s_R^{1/\gamma} s_L - s_L^{1/\gamma} s_R}{s_R^{1/\gamma} - s_L^{1/\gamma}} \tag{52}$$

Wave speeds that satisfy Riemann invariants

$$\lambda^- = \frac{\rho_{*,L} u_* - \rho_L u_L}{\rho_{*,L} - \rho_L}, \quad \lambda^+ = \frac{\rho_R u_R - \rho_{*,R} u_*}{\rho_R - \rho_{*,R}} \tag{53}$$

Implementation

- Reconstruct isentropic system $(\rho, \rho u, S)$
- Compute $\sum_{k=1}^{N} |\lambda^k_{i+1/2}| \alpha^k_{i+1/2} \vec{r}^k_{i+1/2}$ for $(\rho, \rho u, S)$ components
- For energy component:
  $|\lambda^-|(E_{*,L} - E_L) + |u_*|(E_{*,R} - E_{*,L}) + |\lambda^+|(E_R - E_{*,R})$

Positivity conserving while resolving contacts down to vacuum limit

Outline

1. Governing equations
2. Numerical Formulation
3. Benchmarks
4. Collisional-Radiative Model
5. UTIAS Shocktube Experiments
6. Extensions & ongoing research
7. Moment equations
8. Conclusions

Collisional-Radiative Processes

Processes considered:

$$Ar(i) + e^- \underset{F_{ji}}{\overset{C_{ij}}{\rightleftharpoons}} Ar(j) + e^- \quad \textbf{(54)}$$

$$Ar(i) + Ar(1) \underset{L_{ji}}{\overset{K_{ij}}{\rightleftharpoons}} Ar(j) + Ar(1) \quad \textbf{(55)}$$

$$Ar(i) + e^- \underset{O_i}{\overset{S_i}{\rightleftharpoons}} Ar^+ + e^- + e^- \quad \textbf{(56)}$$

$$Ar(i) + Ar(1) \underset{W_i}{\overset{V_i}{\rightleftharpoons}} Ar^+ + e^- + Ar(1) \quad \textbf{(57)}$$

$$Ar(i) + h\nu_{ij} \underset{A_{ij}}{\overset{(1-\Lambda_{ij})A_{ij}}{\rightleftharpoons}} Ar(j) \quad \textbf{(58)}$$

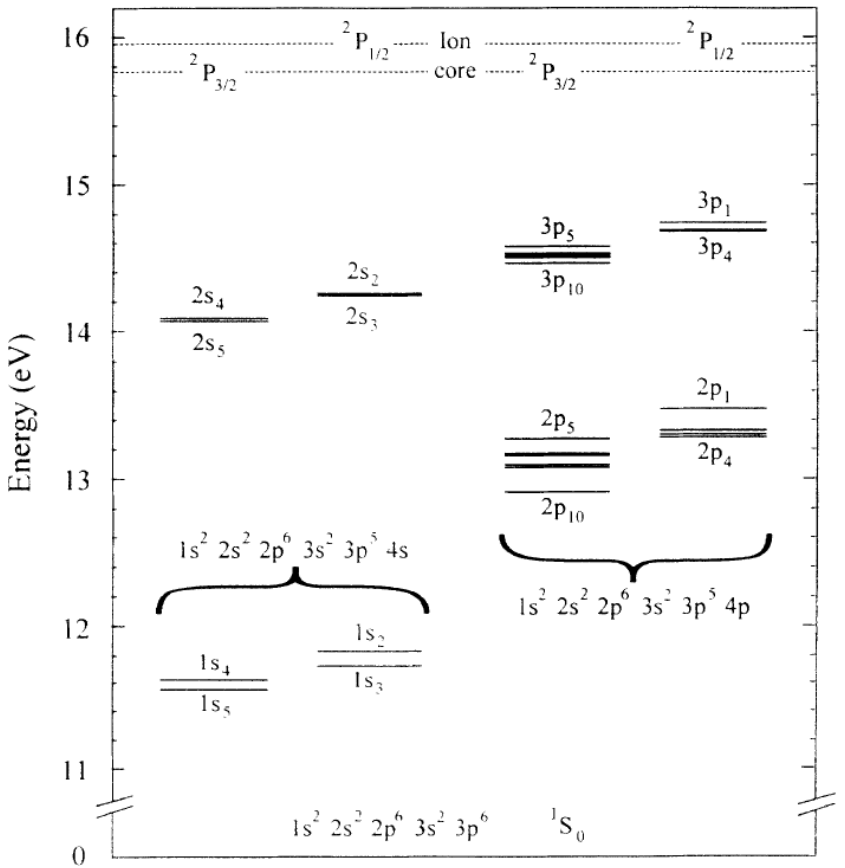
$$Ar(i) + h\nu \underset{R_i}{\overset{(1-\Lambda_i)R_i}{\rightleftharpoons}} Ar^+ + e^- \quad \textbf{(59)}$$

Rate Coeff.	Process
C_{ij}	coll. excitation by electrons
K_{ij}	coll. excitation by g.s. atoms
F_{ji}	coll. de-excitation by electrons
L_{ji}	coll. de-excitation by g.s. atoms
S_i, V_i	coll. ionization
O_i, W_i	three-body recombination
R_i	radiative recombination
A_{ji}	transition probability
Λ_{ji}	bound-bound optical escape factor
Λ_i	bound-free optical escape factor
k_{ei}	electron-ion collisions
k_{en}	electron-neutral collisions
k_{brems}	bremsstrahlung emission

Ground State Argon

Levels

i	$\varepsilon(i)$	g_i	j_c	$n\ell[K]_J$
1	0	1	1.5	$[Mg]3p^6$
2	11.548	5	1.5	$4s[3/2]_2$
3	11.624	3	1.5	$4s[3/2]_1$
4	11.723	1	0.5	$4s'[1/2]_0$
5	11.828	3	0.5	$4s'[1/2]_1$
6	12.907	3	1.5	$4p[1/2]_1$
7	13.076	7	1.5	$4p[5/2]_3$
8	13.095	5	1.5	$4p[5/2]_2$
9	13.153	3	1.5	$4p[3/2]_1$
10	13.172	5	1.5	$4p[3/2]_2$
11	13.273	1	1.5	$4p[1/2]_0$
12	13.283	3	0.5	$4p'[3/2]_1$
13	13.302	5	0.5	$4p'[3/2]_2$
14	13.328	3	0.5	$4p'[1/2]_1$
15	13.480	1	0.5	$4p'[1/2]_0$
16	13.845	1	1.5	$3d[1/2]_0$
17	13.864	3	1.5	$3d[1/2]_1$
⋮				
30	14.255	3	0.5	$3d'[5/2]_3$
31	14.304	3	0.5	$3d'[3/2]_1$
∞	15.760	4	1.5	$[Mg]3p^5$
∞'	15.937	2	0.5	$[Mg]3p^5$



Determination of Reaction Rates

Maxwellian electron energy distribution function:

$$f(\varepsilon)\ d\varepsilon = \frac{2}{\pi^{1/2}} \frac{\varepsilon^{1/2}}{(kT_e)^{3/2}} e^{-\varepsilon/kTe}\ d\varepsilon, \quad \int_0^\infty f(\varepsilon)\ d\varepsilon = 1 \tag{60}$$

Assumption is valid if $1/(\bar{\nu}_{ee}\tau) \ll 1$ **and** $\bar{C}_e/(\bar{\nu}_{ee}L) \ll 1$.

Species Production Rates

Forward rates:

$$k = \frac{\bar{v}}{(kT)^2} \int_{\varepsilon_o}^\infty \sigma(\varepsilon)\varepsilon e^{-\varepsilon/k_B T}\ d\varepsilon, \quad \bar{v} = \sqrt{\frac{8kT}{\pi\mu}} \tag{61}$$

Reverse rates via detailed balance:

$$k_{ji} = k_{ij} \frac{g_i}{g_j} e^{\varepsilon_{ij}/kT} \tag{62}$$

$$k_r = k_i \frac{g_i}{2g_+} \frac{V}{Z} \tag{63}$$

$$Z = Z_{\textbf{trans},e} \cdot Z_{\textbf{el}} \tag{64}$$

$$= \left(\frac{2\pi m_e k_B T_e}{h^2}\right)^{3/2} V \cdot e^{-\varepsilon_i/k_B T} \tag{65}$$

Energy Production Rates

Energy moment:

$$k' = \frac{\bar{v}}{(k_B T)^2} \int_{\varepsilon_o}^\infty \sigma(\varepsilon)\varepsilon^2 e^{-\varepsilon/k_B T}\ d\varepsilon \tag{66}$$

Used to compute energy change due to free-bound processes (photorecombination)

Outline

1 Governing equations

2 Numerical Formulation

3 Benchmarks

4 Collisional-Radiative Model

5 UTIAS Shocktube Experiments

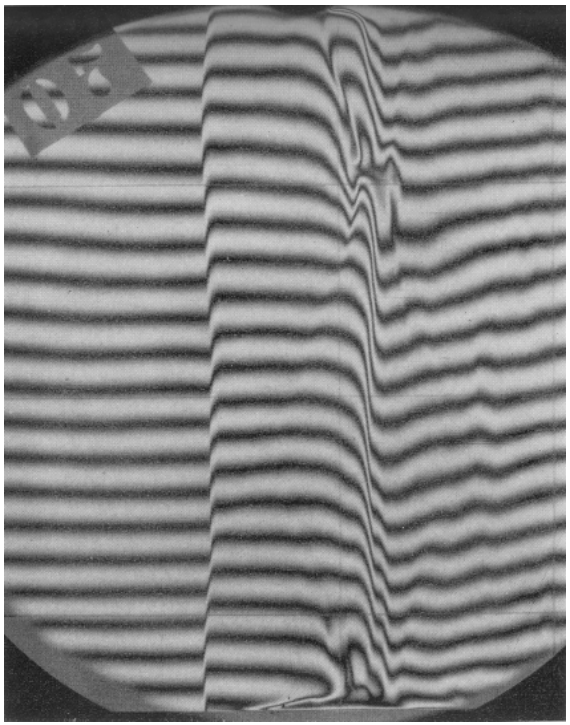
6 Extensions & ongoing research

7 Moment equations

8 Conclusions

UTIAS Ionizing Shock Experiments

- Measurements were taken in the form of interferograms from which the total mass and electron number densities were derived
- Key parameters for describing the shock structure can be ascertained, including the peak ionization fraction, α, number density, n, and the relaxation length, ℓ



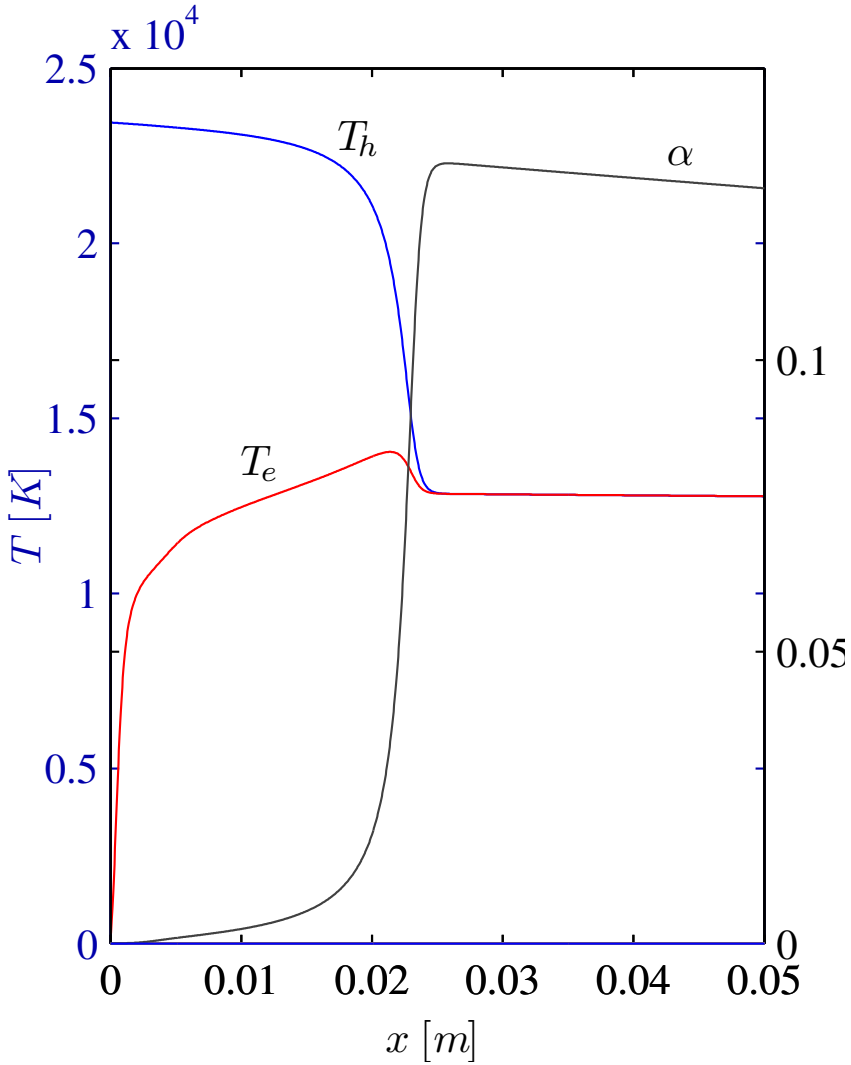
UTIAS Cases, Glass and Liu (1978)

Cases studied by Glass and Liu

Case	Ma_s	p_o [torr]	T_o [K]	α
1	15.9	5.14	293.6	0.14
2	16.1	5.15	295.9	0.15
3	16.5	5.12	296.6	0.16
4	13.0	5.01	296.6	0.06
7	14.7	4.08	297.8	0.106

Relaxation length

Case	ℓ [cm] Experiment	Theory
1	2.00	2.09
2	1.90	1.88
3	1.80	1.61
4	8.90	10.6
7	4.40	4.48



Steady-State Governing Equations

Removing the time-dependency from the governing equations,

$$\cancelto{0}{\frac{\partial Q}{\partial t}} + A\frac{\partial F}{\partial x} = \dot{\Omega}, \tag{67}$$

reduces system to a set of quasi-linear ODE's,

$$\frac{dQ}{dx} = A^{-1}\dot{\Omega} \tag{68}$$

Equivalently:

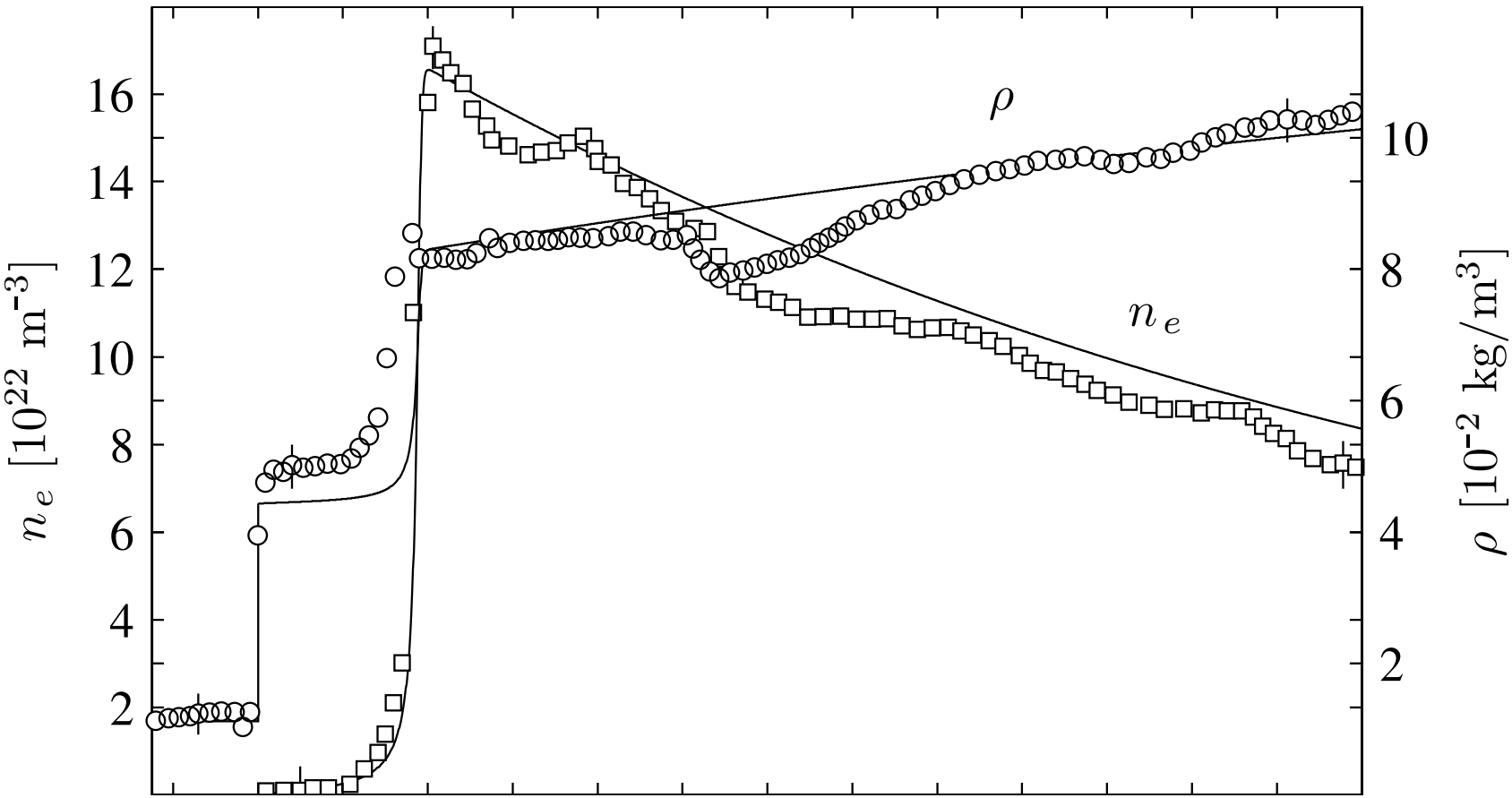
$$\frac{dQ}{dx} = R\Lambda^{-1}L\dot{\Omega} \tag{69}$$

Implicit numerical formulation

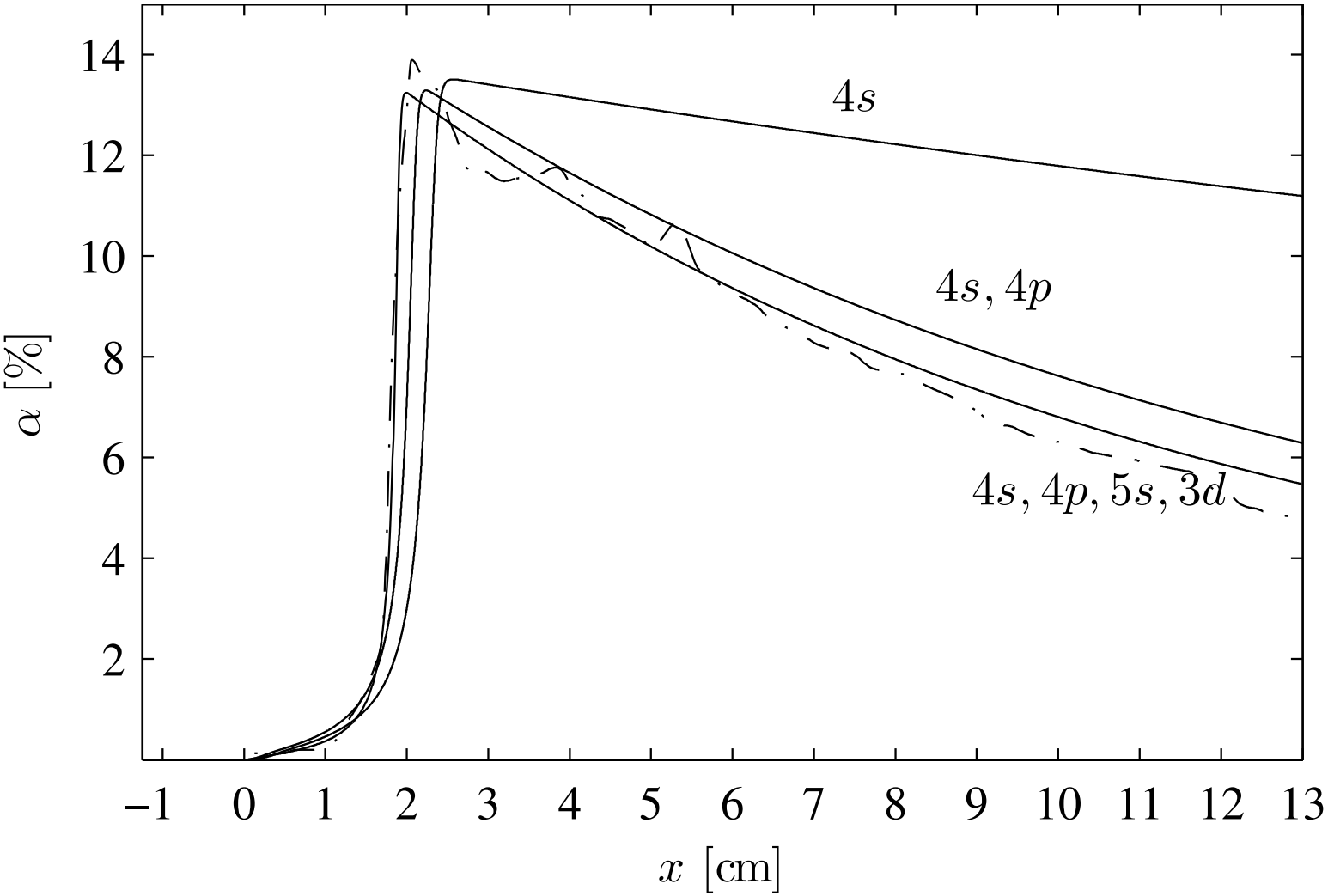
$$\Delta Q = \left[I - \Delta x A^{-1}\left(\frac{\partial \dot{\Omega}}{\partial Q} - \frac{\partial A}{\partial Q}A^{-1}\dot{\Omega}\right)\right]^{-1}\Delta x A^{-1}\dot{\Omega} \tag{70}$$

Initial conditions given by Rankine-Hugoniot jump conditions.

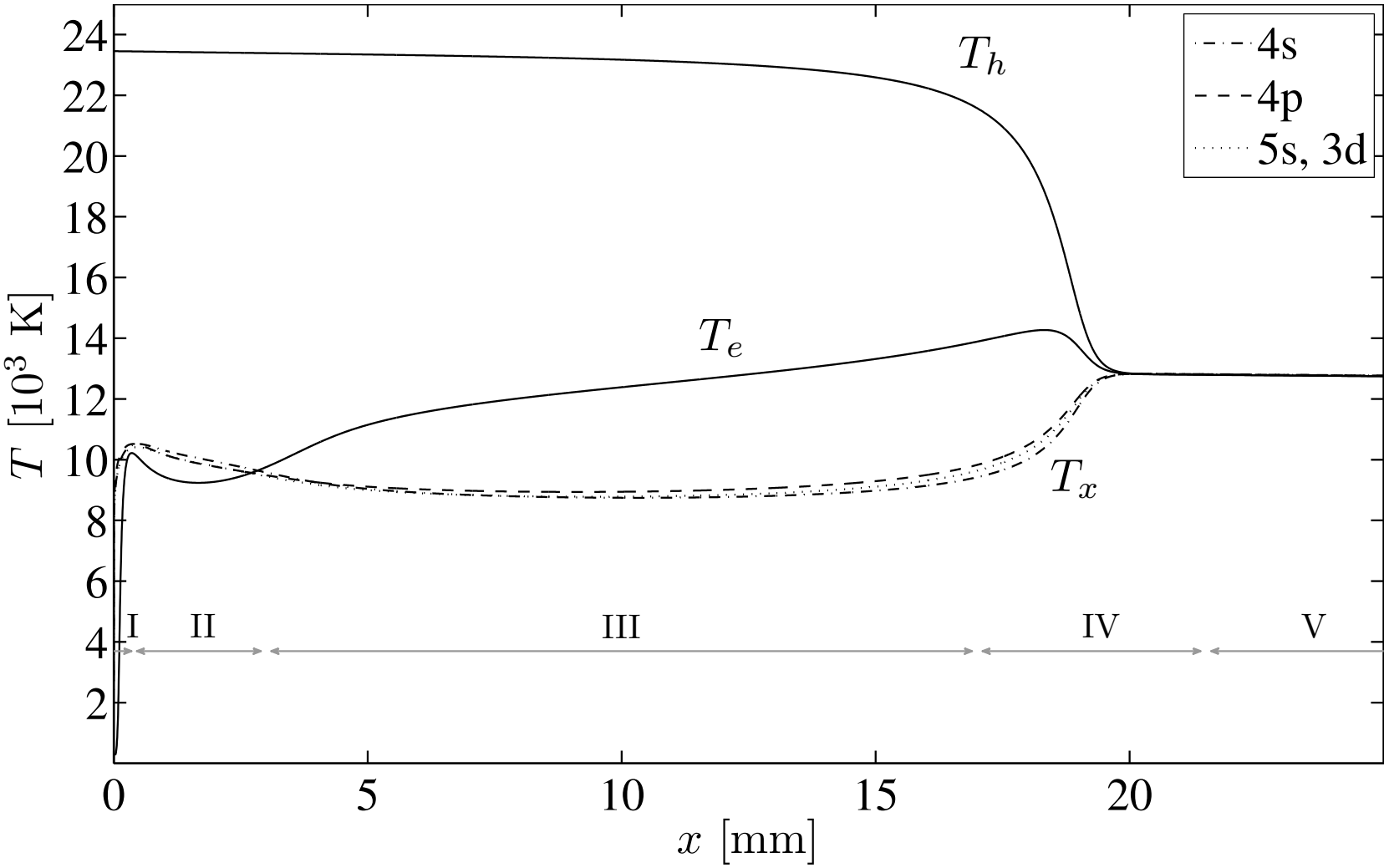
Case 1, Ma 15.9: Experimental vs. model



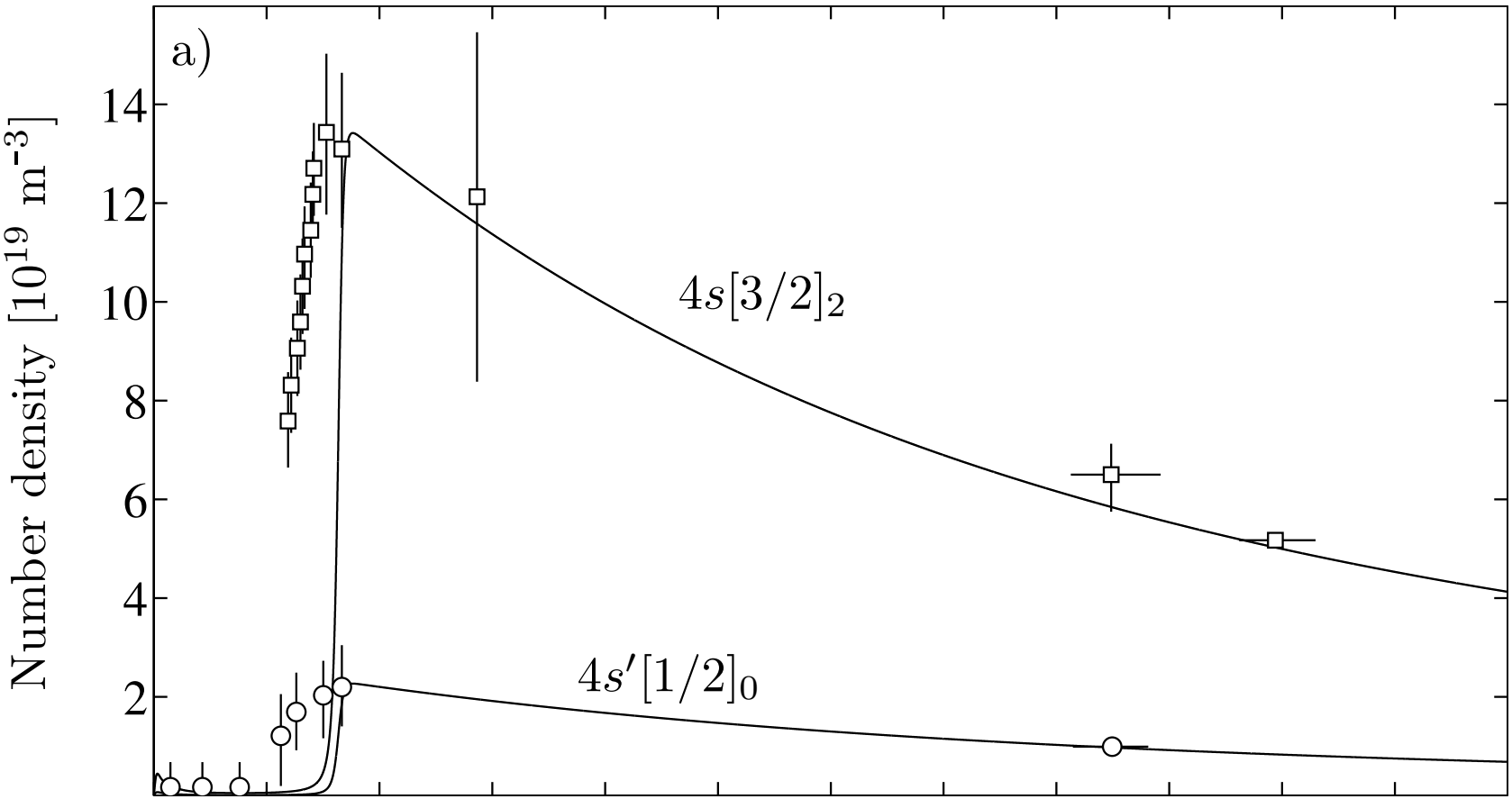
Case 1, Ma 15.9: Effect of higher levels



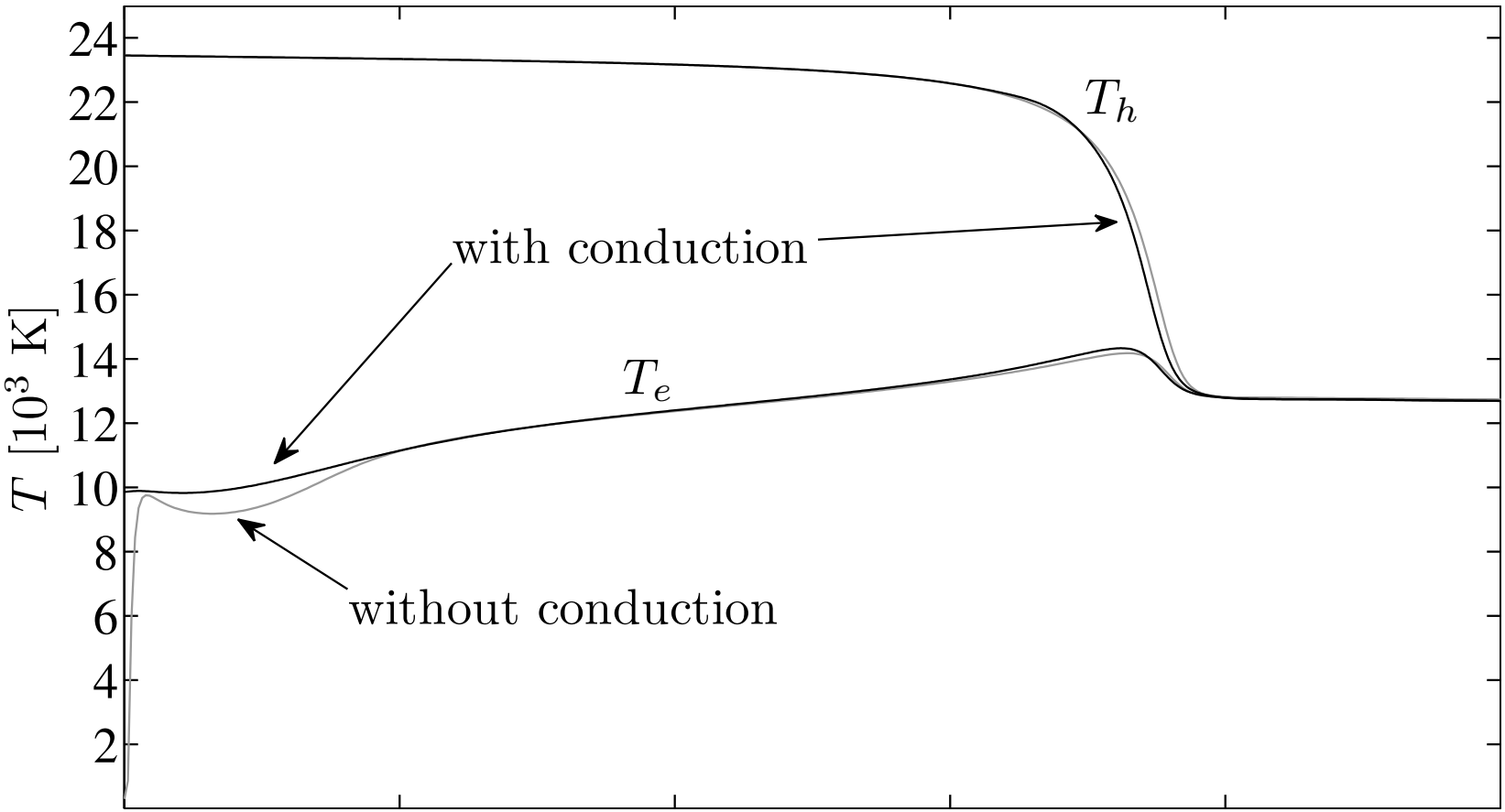
Case 1, Ma 15.9: Internal structure



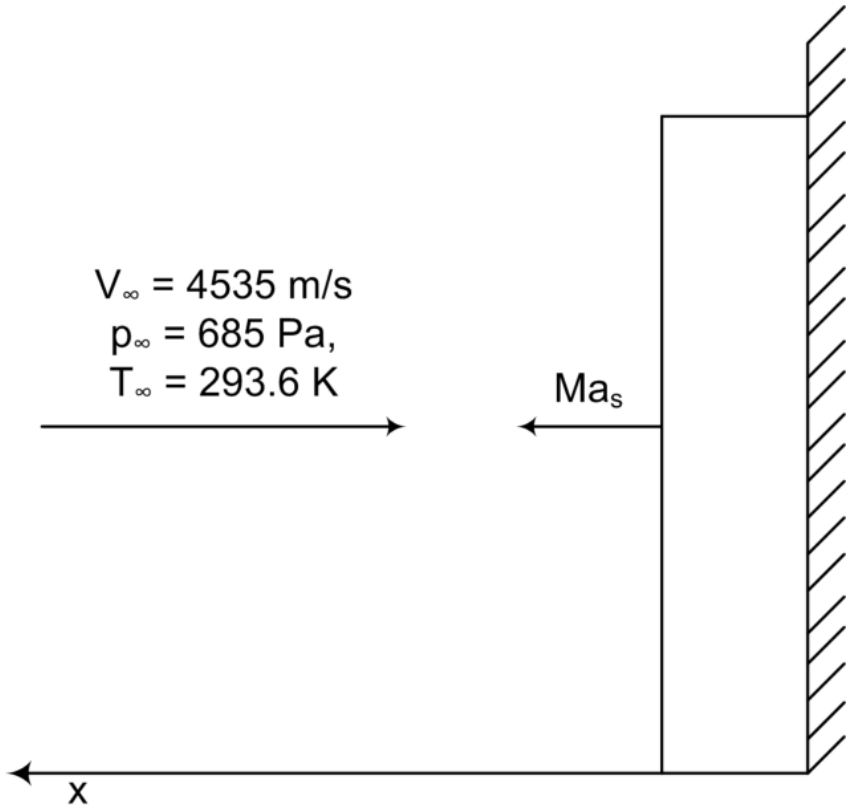
Metastable Population: Houwing et al. (1983)



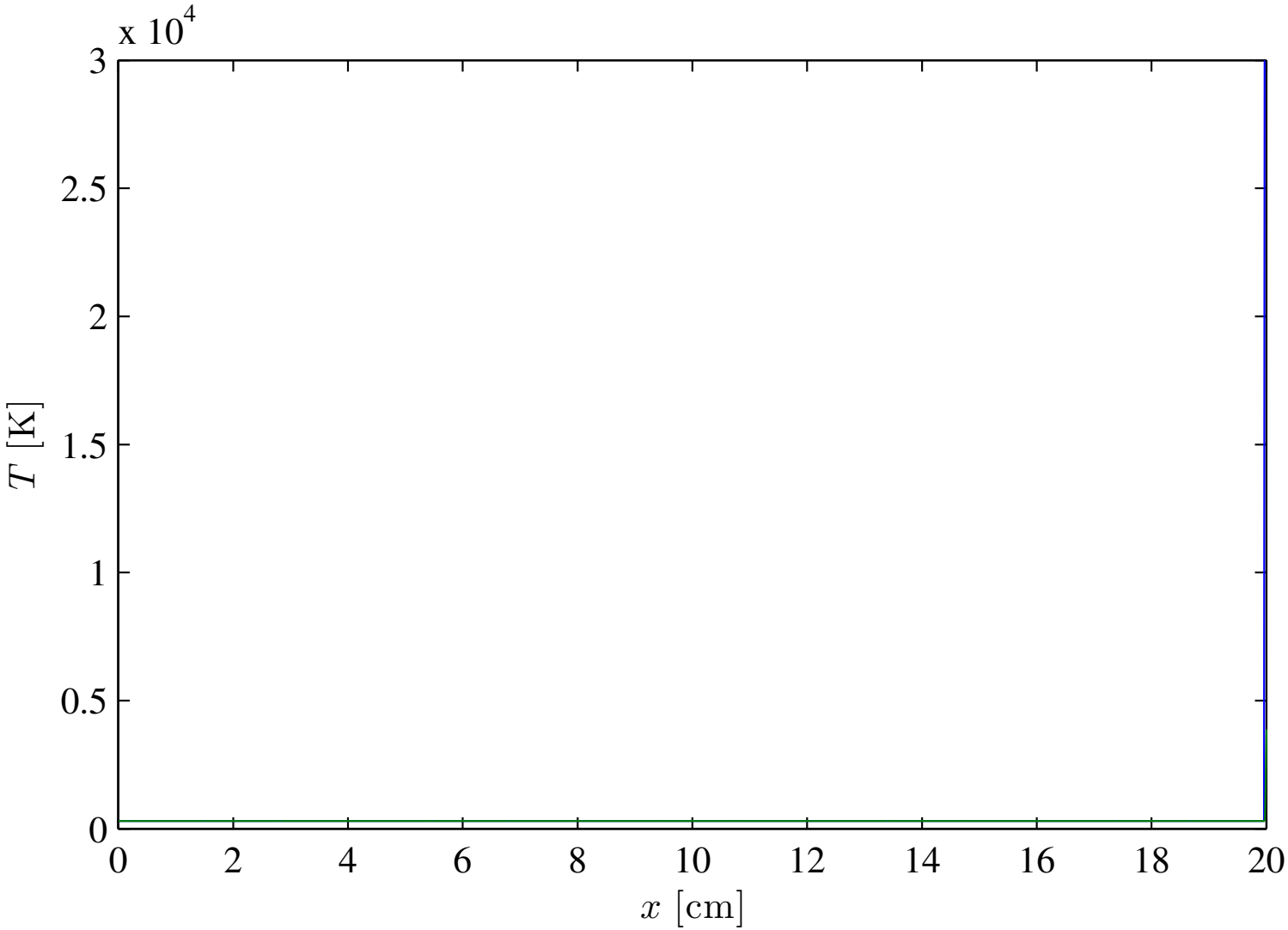
Electron Heat Conduction



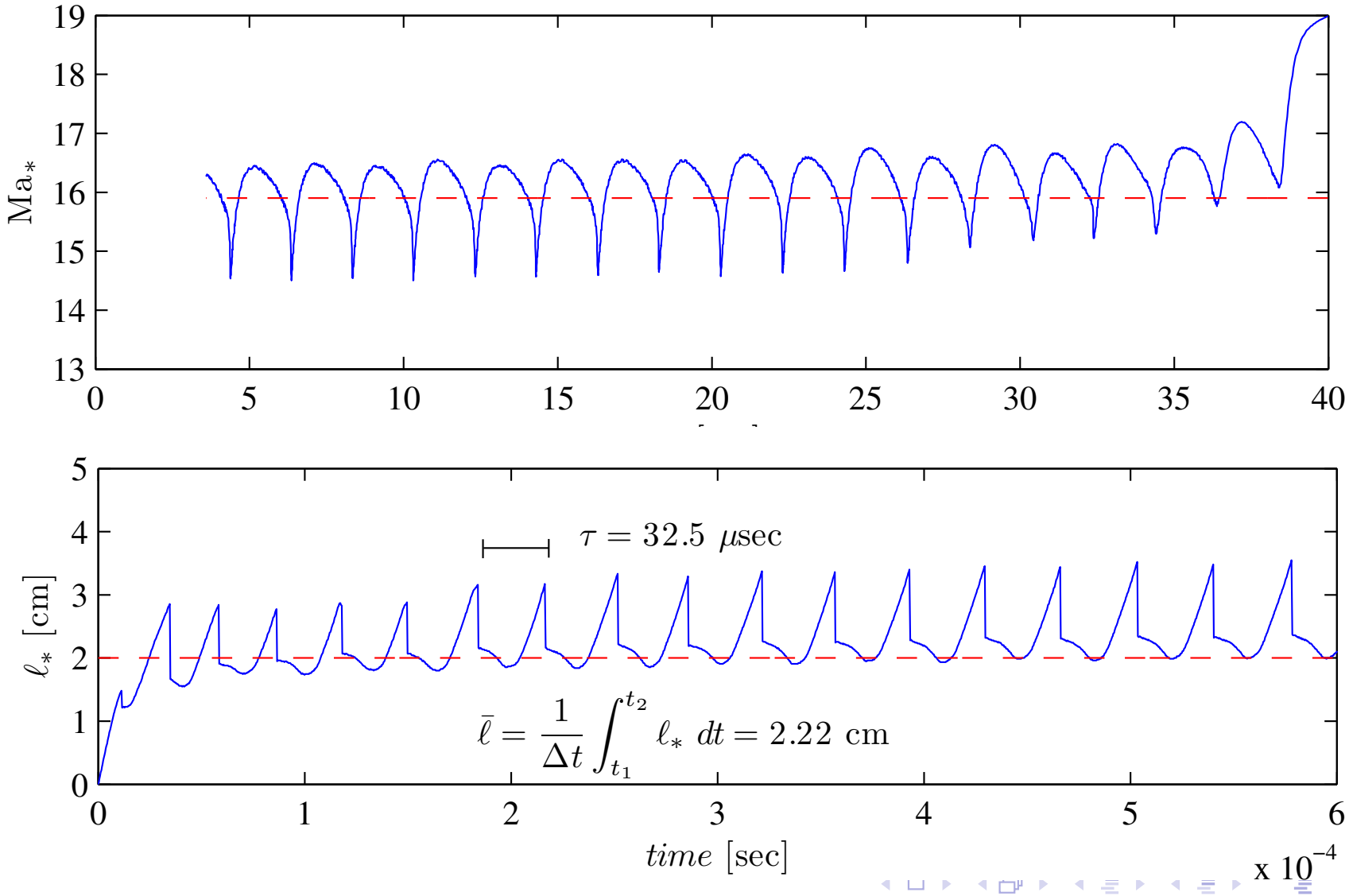
Unsteady 1D Simulations



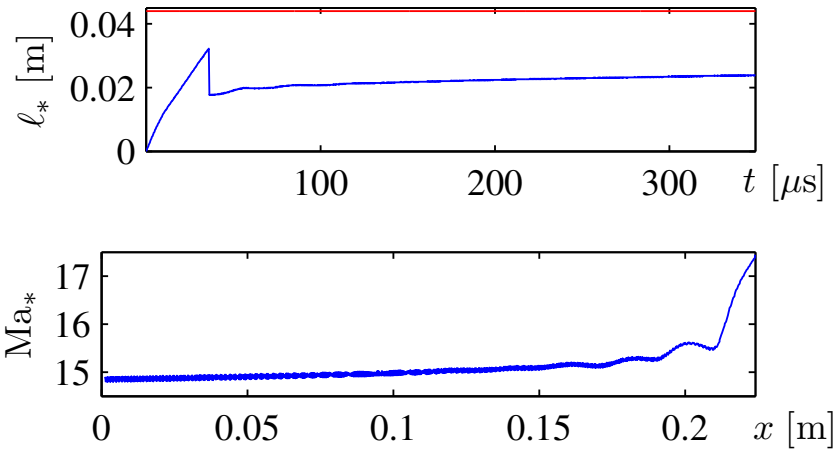
Case 1: Mach 15.9

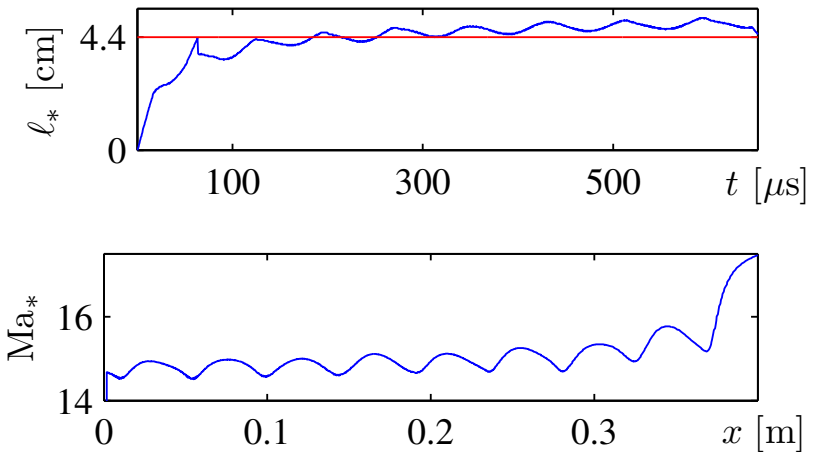


Instantaneous Mach Number and Induction Length



Sensitivity to Kinetics

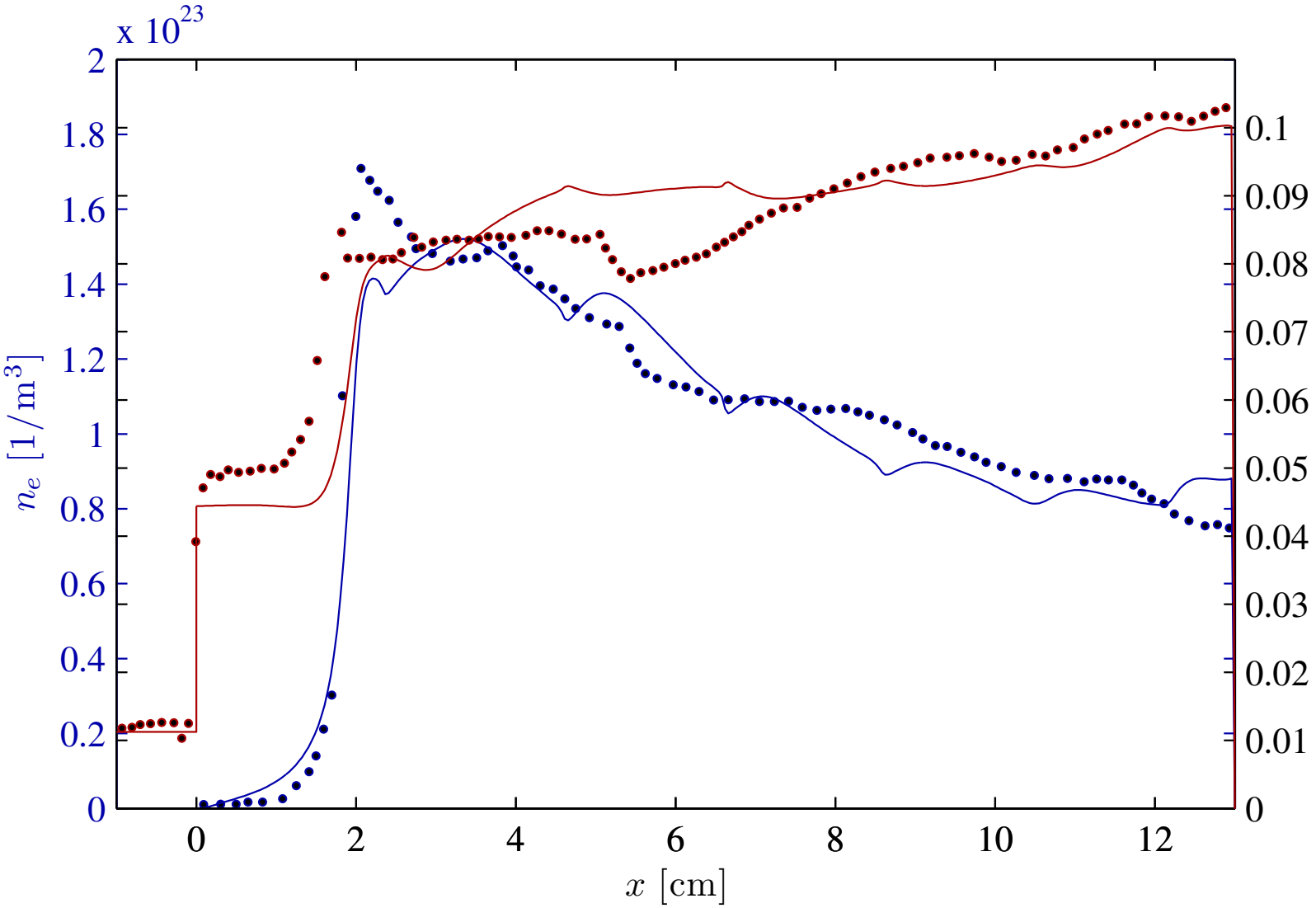




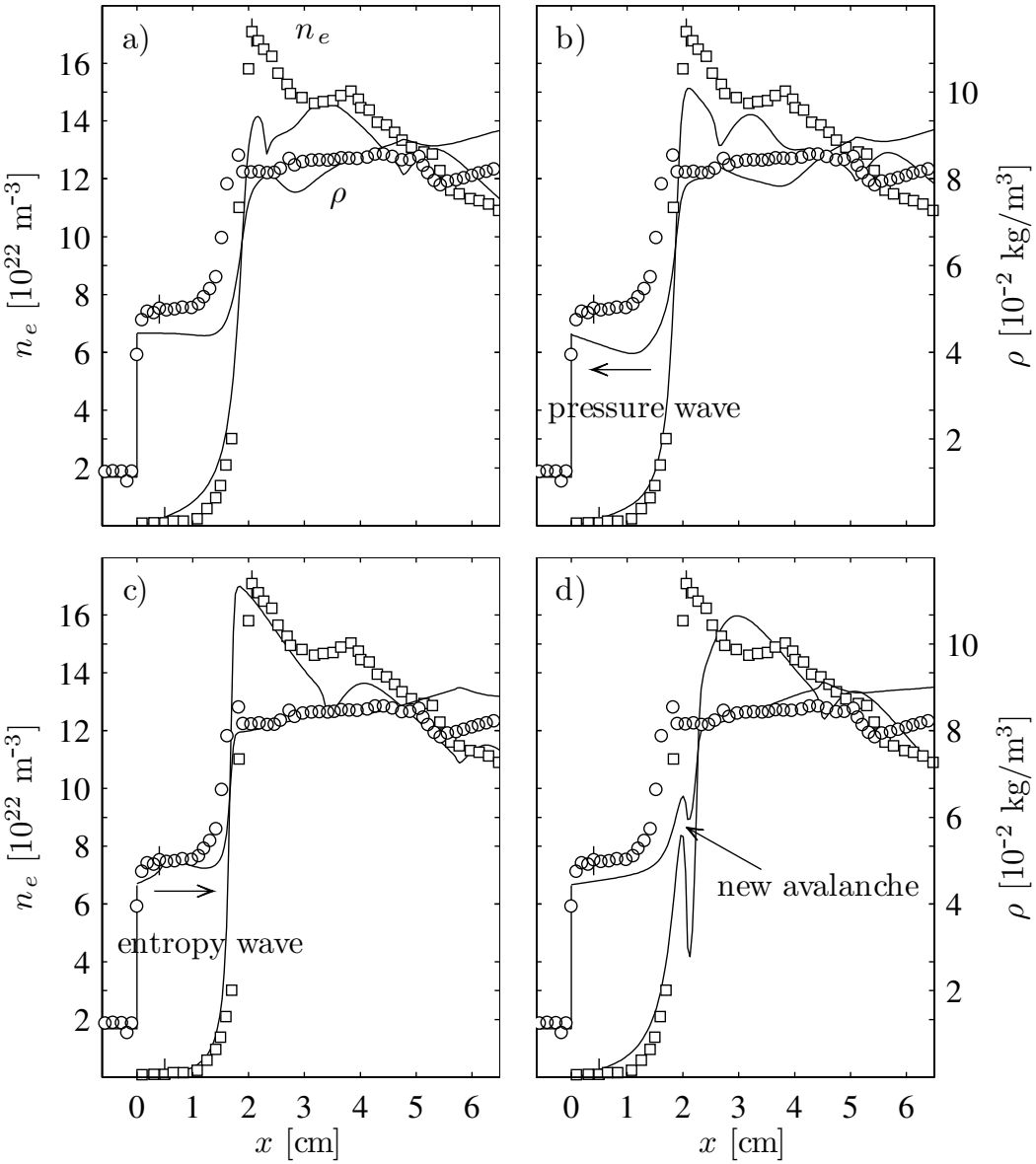
- Increase in atom-atom excitation cross sections leads to damping of fluctuations in the shock speed
- In this case, self-sustaining oscillations cannot be achieved
- Energy is diverted to atom-atom excitation and ionization rather than increasing the shock temperature
- These cross sections also have large effect on relaxation length

- Reduction in electron-atom excitation cross sections leads to damping of the pressure oscillations between the electron avalanche and the shock front
- This slows the rate of onset of the avalanche and gives fluid more time to 'react' to kinetics
- Discontinuous shift in relaxation length has been eliminated

Case 1: Mach 15.9

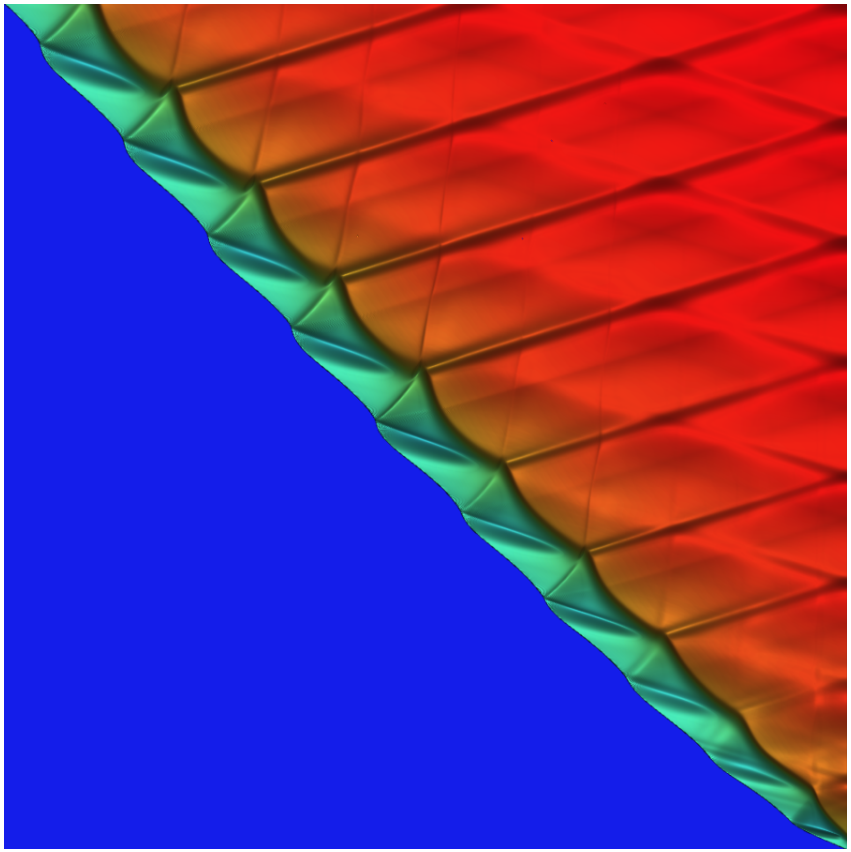


Dynamic evolution

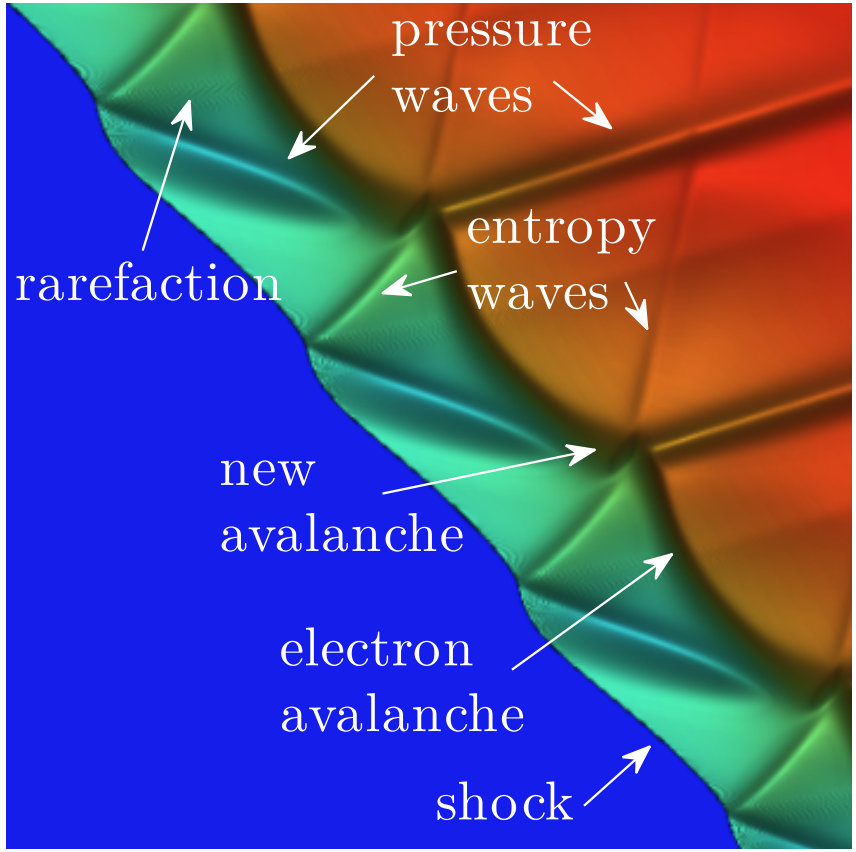


Space-time plots

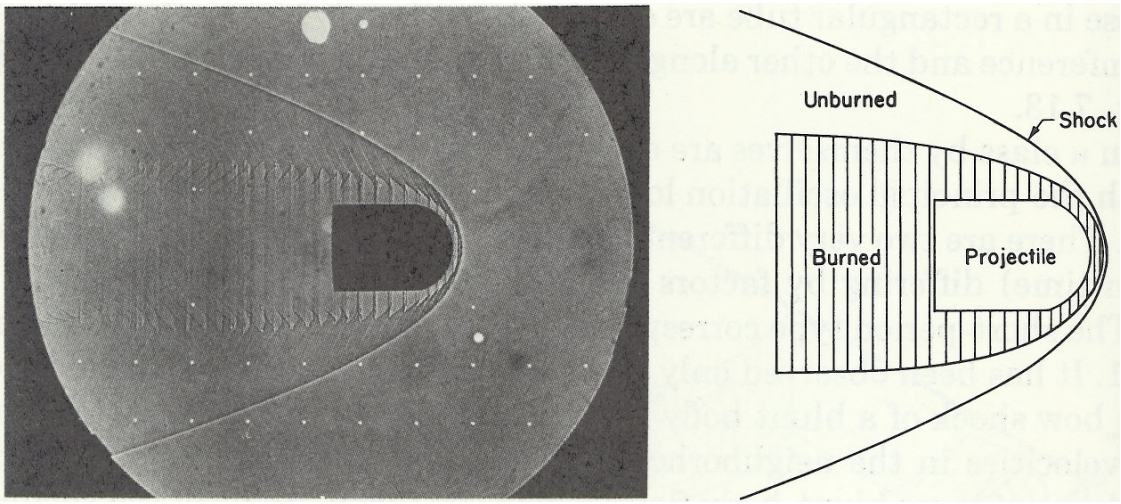
Density

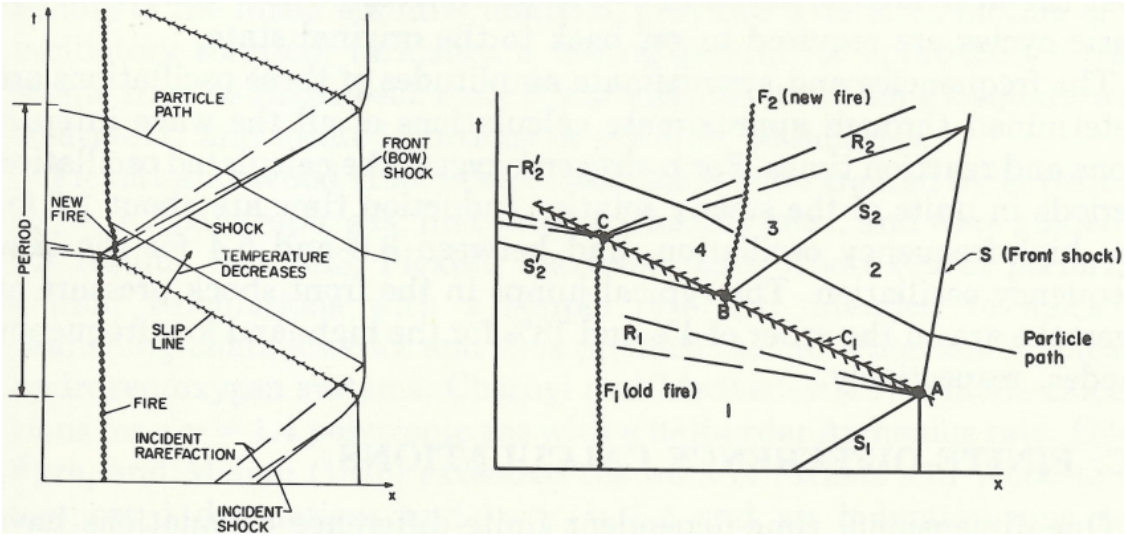


Density

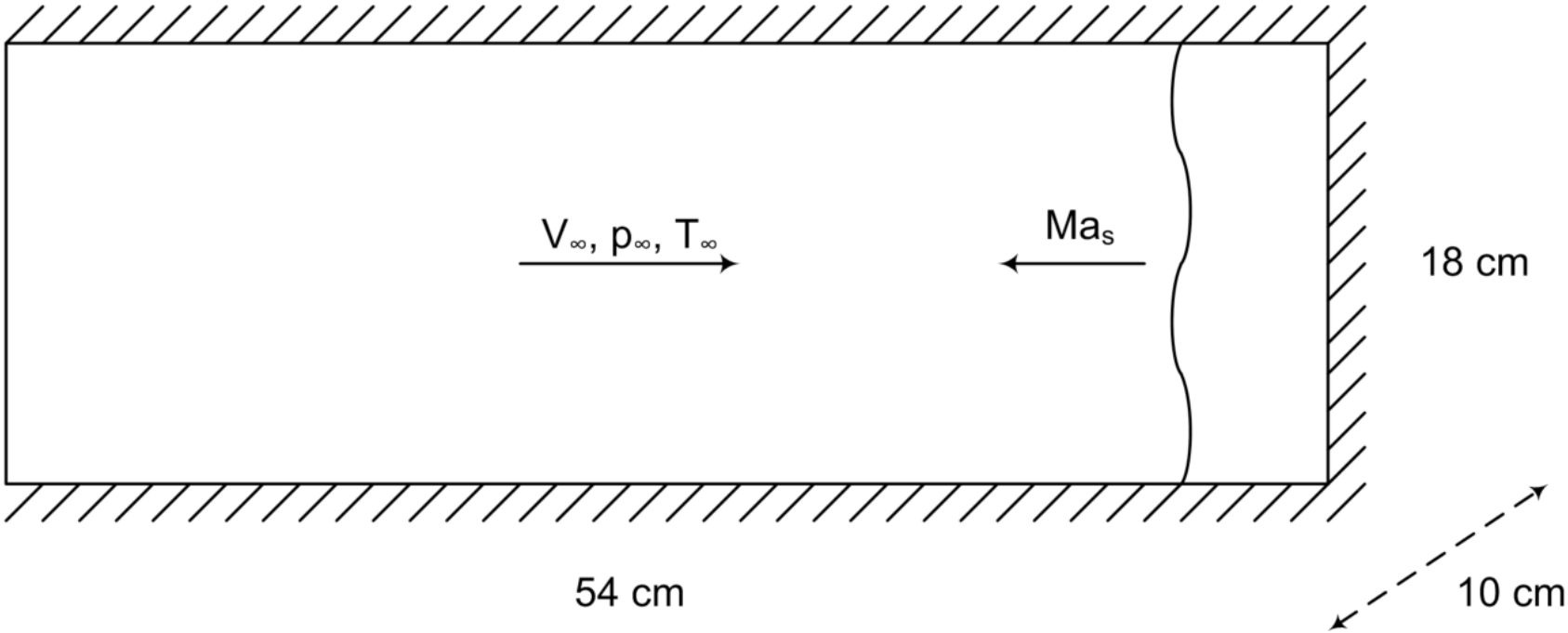


Analogy to shock-induced combustion (Lehr 1971, Wilson 1991)





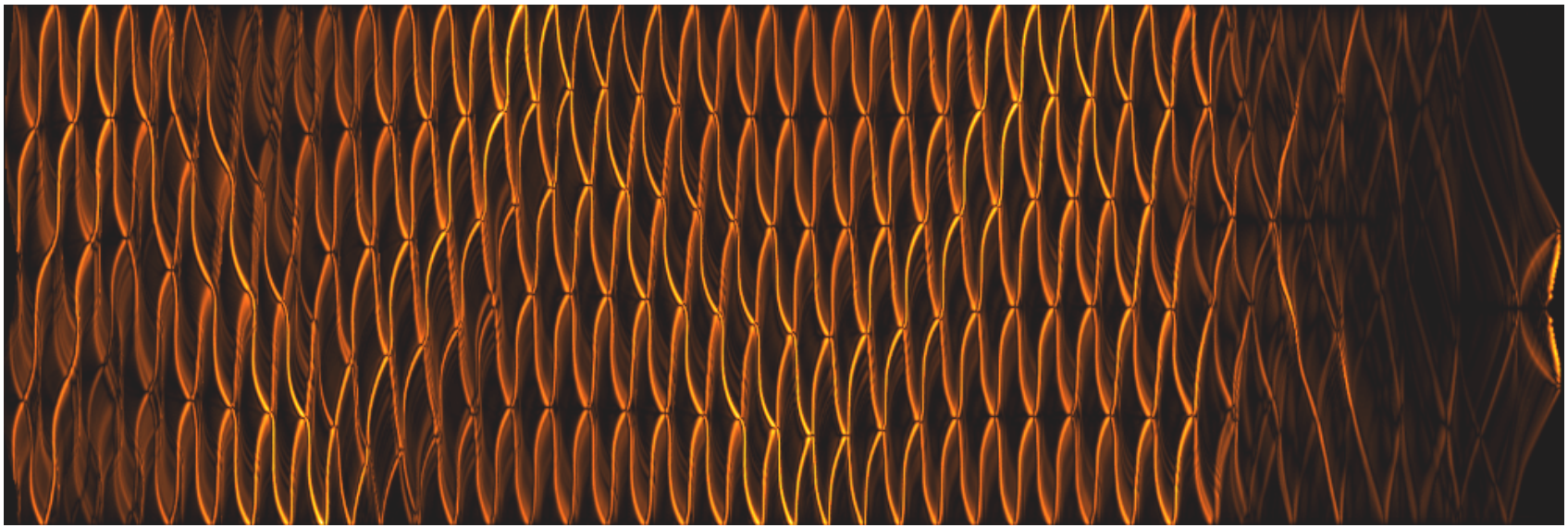
Two-Dimensional Numerical Setup



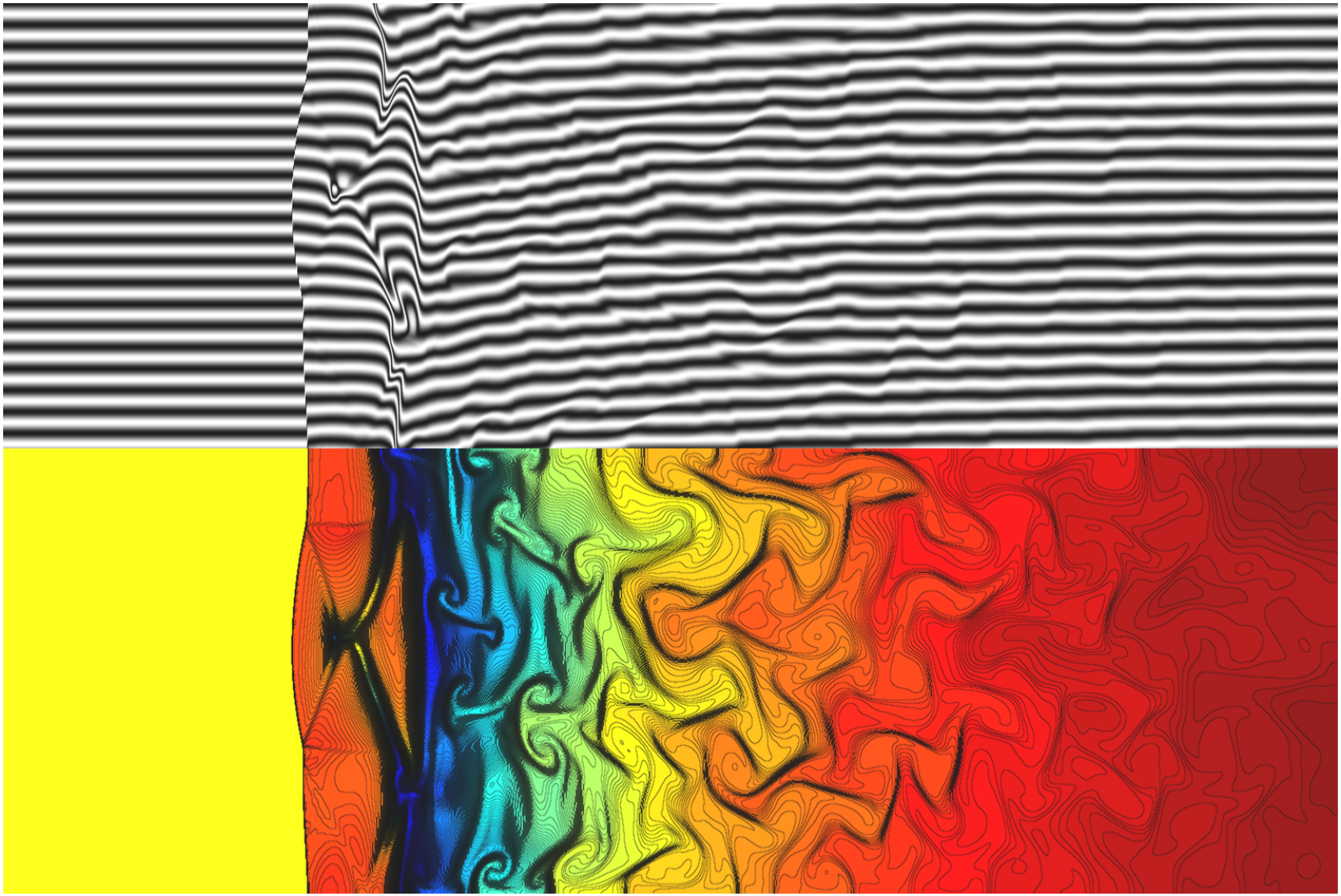
Two-Dimensional Results Mach 16.5

Soot Trace

Numerical soot trace computed from flow vorticity: $\nabla \times \vec{u}$
Maximum vorticity occurs at triple points, due to shearing of the flow.

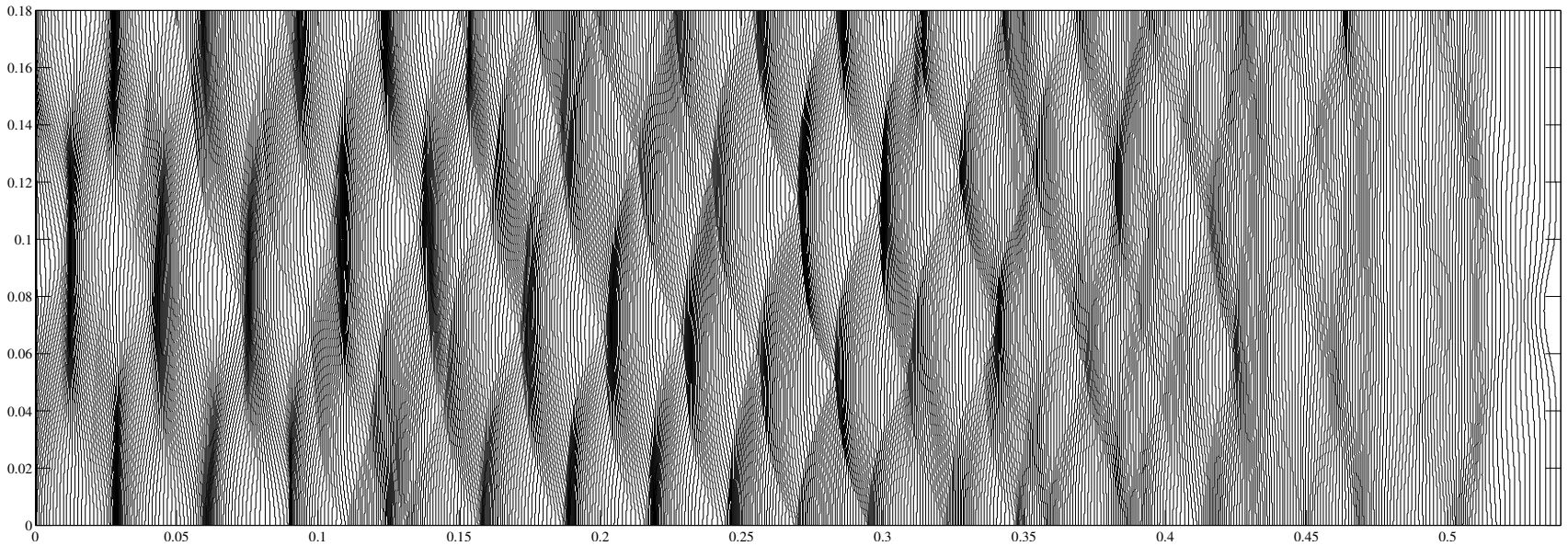


Two-Dimensional Results Mach 14.7



Mach 14.7

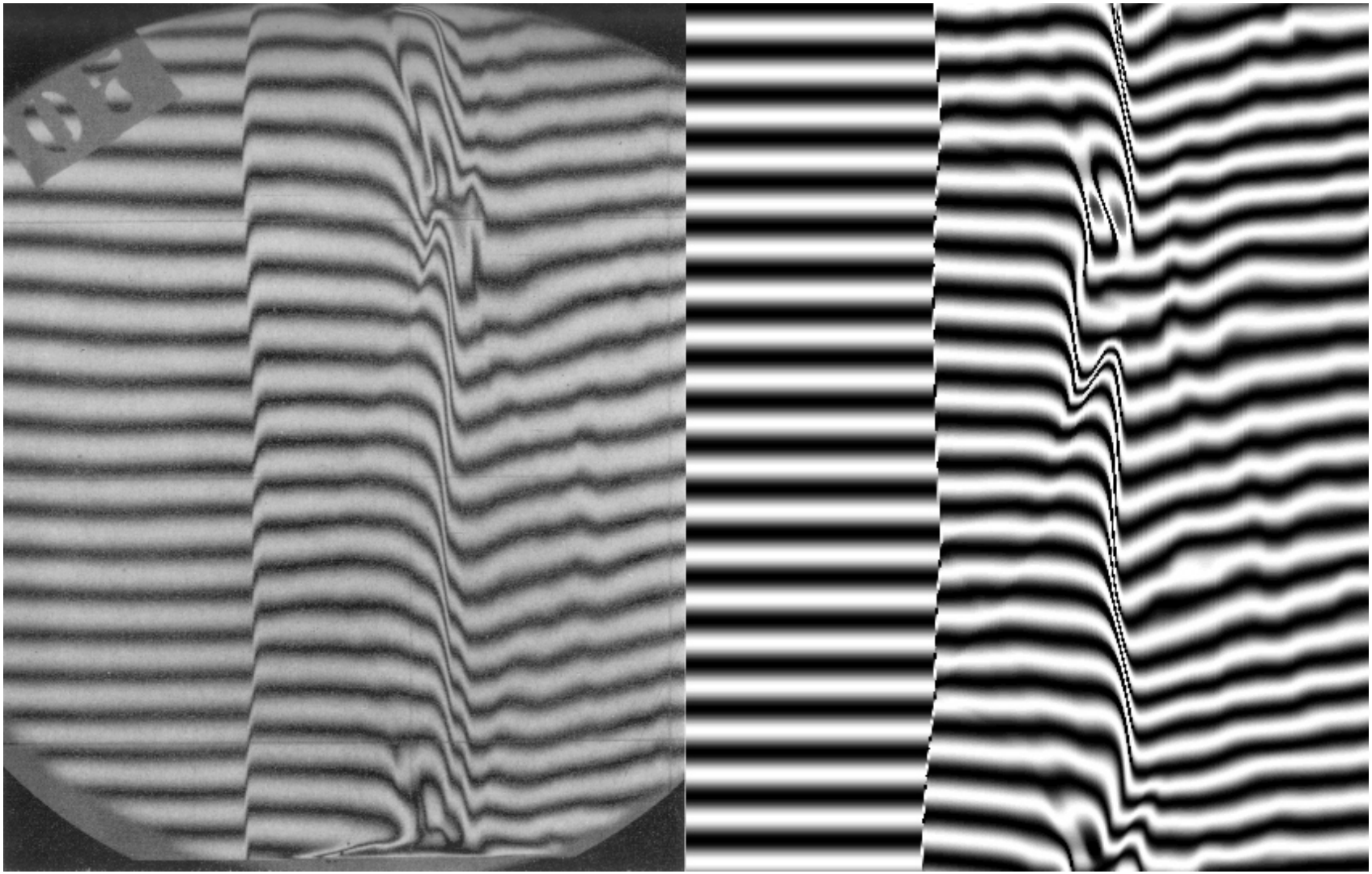
Numerical soot trace visualized by snapshots of instantaneous shock fronts



Cell width ≈ 12 cm $\rightarrow 1.5$ cells per channel width.
Decaying Mach number leads to changes in resonance and cell pattern.

Mach 14.7

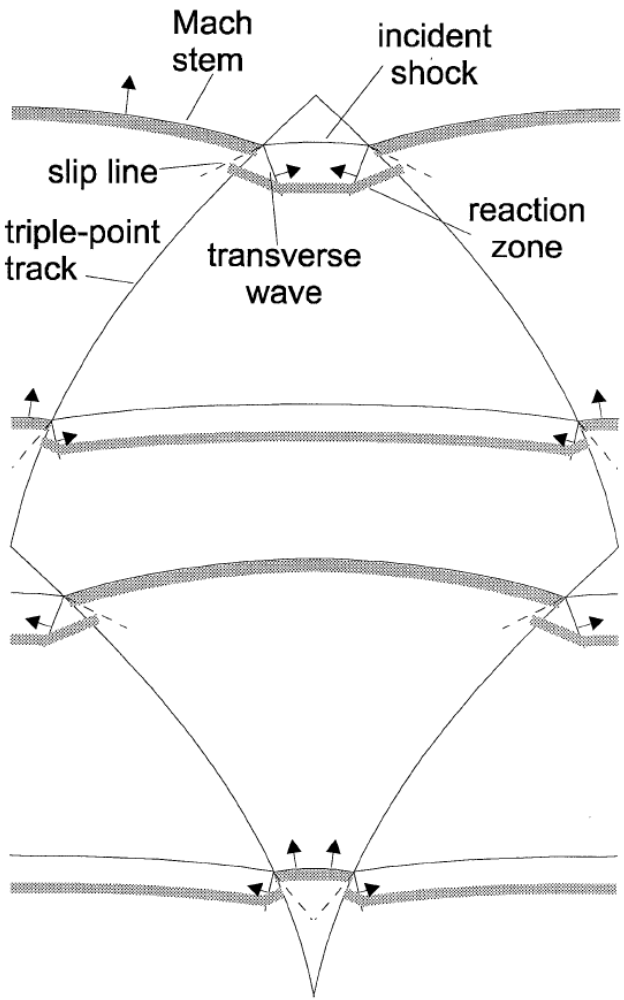
Direct comparison with experiment shows excellent agreement

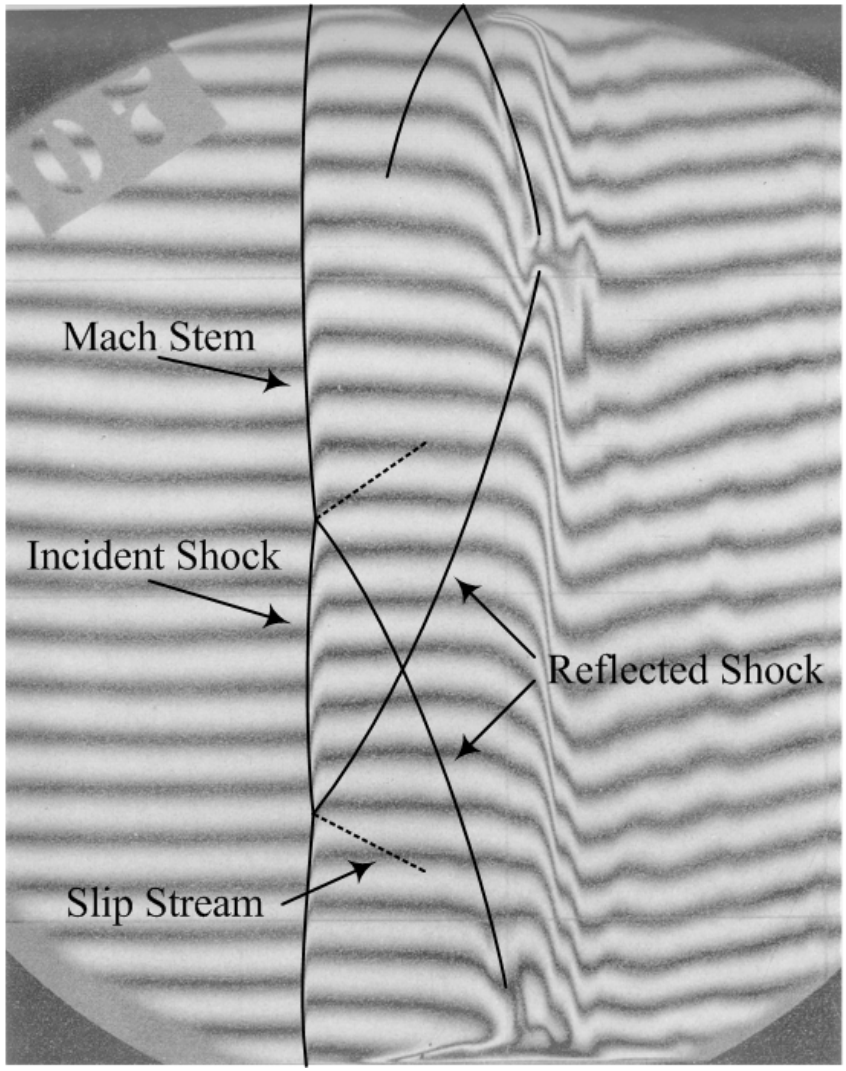


Missing piece is viscous boundary layer.

Detonation/Ionization cell analog

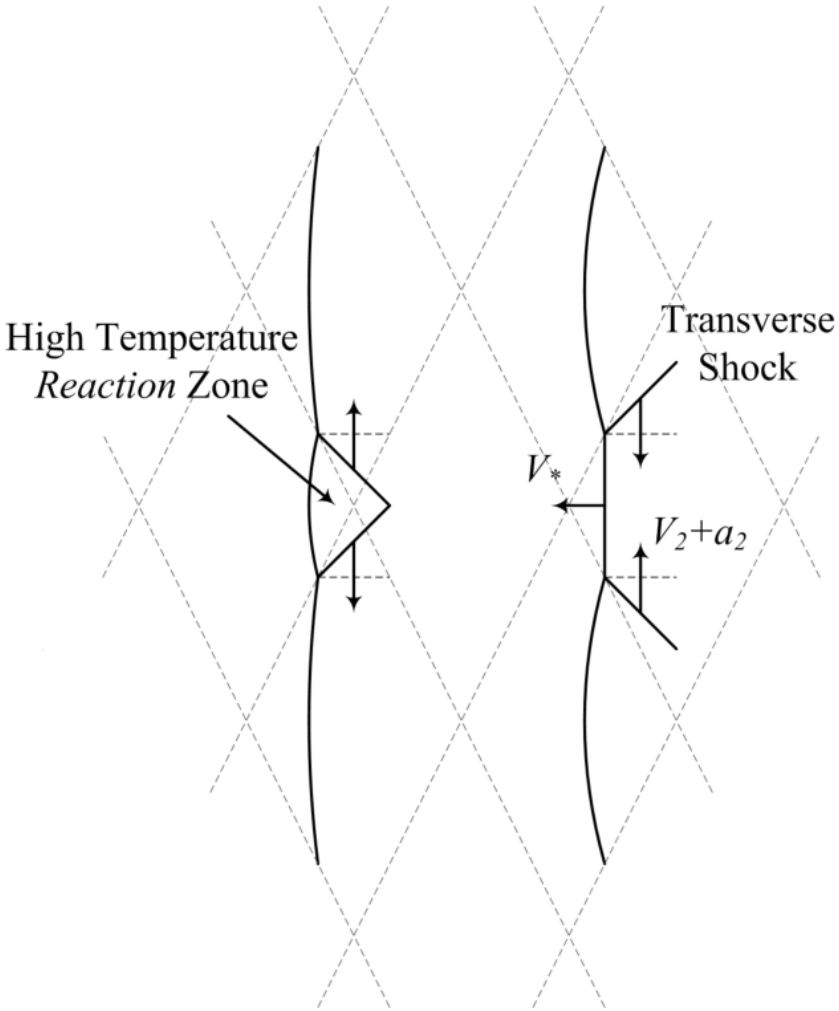
Ionization analog to detonation cells:





Cell Structure

- Transverse shock waves compress and heat gas, rapidly increasing ionization
- High temperarature region is essentially an 'initiation' region



Outline

1 Governing equations

2 Numerical Formulation

3 Benchmarks

4 Collisional-Radiative Model

5 UTIAS Shocktube Experiments

6 Extensions & ongoing research

7 Moment equations

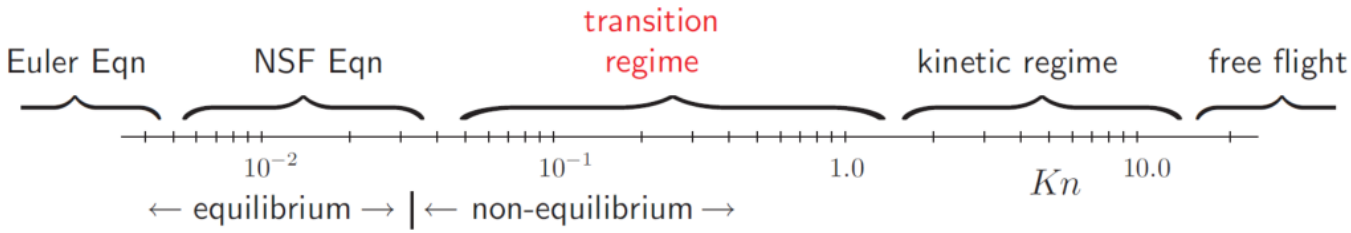
8 Conclusions

Outline

1. Governing equations
2. Numerical Formulation
3. Benchmarks
4. Collisional-Radiative Model
5. UTIAS Shocktube Experiments
6. Extensions & ongoing research
7. Moment equations
8. Conclusions

13 Moment Equations

- insufficient number of particle collisions may lead to nonequilibrium
- nonequilibrium important in rarefied situations
- scaling based on Knudsen number: $\mathrm{Kn} = \frac{\text{mean-free path}}{\text{observation length}}$

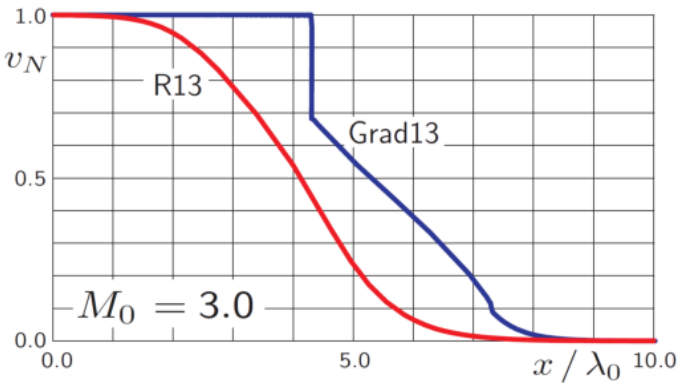


$$Q = \begin{pmatrix} \rho \\ \rho u \\ 3p + \rho u^2 \\ 3\pi + 2\rho u^2 \\ 2q + 5pu + 2\pi u + \rho u^3 \end{pmatrix}$$

$$F = uQ + \begin{pmatrix} 0 \\ p + \pi \\ 2pu + 2\pi u + 2q \\ 4pu + 4\pi u + \frac{8}{5}q \\ 3pu^2 + 3\pi u^2 + \frac{22}{5}qu + \frac{p}{\rho}(5p + 7\pi) \end{pmatrix}$$

$$\Omega = \begin{pmatrix} 0 \\ 0 \\ 0 \\ -\nu\pi - m_{xxx} \\ -\nu(\pi u + 2/3q) - R_{xx} \end{pmatrix}$$

- regularization leads to smooth shock
  Torrilhon/Struchtrup (2004)



Different models for different flow regimes

- Validity of the models

Flow regime	**Knudsen number**	**Kinetic eqs.**	**Boltzmann moment systems**	**Navier -Stokes eqs.**
Rarefied	$1 \leq Kn$	✓	–	–
Transition	$10^{-2} \leq Kn < 1$	✓	✓	–
Continuum	$Kn < 10^{-2}$	✓	✓	✓

- In the transition and continuum regimes
  - Solving kinetic eqs. by DSMC methods is expensive
  - Solving Boltzmann moment systems by CFD methods is more efficient

$\Rightarrow$ Optimal choice for hybrid numerical scheme

- Boltzmann moment systems for the continuum and transition regimes
- Kinetic eqs. for the rarefied regime

Eigenvalues

The eigenvalues of $\mathbf{A_p}$, in increasing order, have been found to be

$$\lambda = \{u - c_f^-, u - c_s^-, u, u + c_s^+, u + c_f^+\}$$

where $u \pm c_f^\pm$ and $u \pm c_s^\pm$ are the speeds of the *fast* and *slow* nonlinear waves that are given by

$$c_f^\pm = \sqrt{c_2} + \sqrt{c_1 - c_2 \pm \frac{24}{25}\frac{q}{\rho\sqrt{c_2}}} \tag{71}$$

and

$$c_s^\pm = \sqrt{c_2} - \sqrt{c_1 - c_2 \pm \frac{24}{25}\frac{q}{\rho\sqrt{c_2}}}, \tag{72}$$

respectively, where

$$c_1 = \frac{39p + 31\pi}{15\rho}, \quad c_2 = \frac{1}{3}c_1 + \frac{\sqrt{2b}}{45\rho}\cos\left(\frac{1}{3}\cot^{-1}\frac{d}{\sqrt{50b^3 - d^2}}\right) \tag{73}$$

$$b = 1773p^2 + 3234p\pi + 1898\pi^2, \tag{74}$$

$$\text{and} \quad d = 209952\rho q^2 + 5(39p + 31\pi)(2277p^2 + 4866p\pi + 3772\pi^2). \tag{75}$$

Hyperbolicity Limit

Hyperbolicity limit can be determined from characteristic polynomial (Müller and Ruggeri, 1998):

$$(225 + 450\kappa + 315\kappa^2) - 288\eta\lambda - 10(39 + 31\kappa)\lambda^2 + 75\lambda^4 = 0 \quad (76)$$

where

$$\eta = \frac{q}{\rho T^{3/2}} \quad \text{and} \quad \kappa = \frac{\pi}{\rho T} \quad (77)$$

We arrive at the same limit based on $50b^3 - d^2 > 0$ (from Eq. (73)),

$$\begin{aligned} 125(5 + 10\kappa + 7\kappa^2)(423 + 534\kappa + 8\kappa^2)^2 \\ - 2880(39 + 31\kappa)(2277 + 4866\kappa + 3772\kappa^2)\eta^2 \\ - 60466176\eta^4 > 0 \end{aligned} \quad (78)$$

Mach 1.1 Shock with 13 Moment Equations

Third-order finite volume solution using Roe's flux-difference splitting

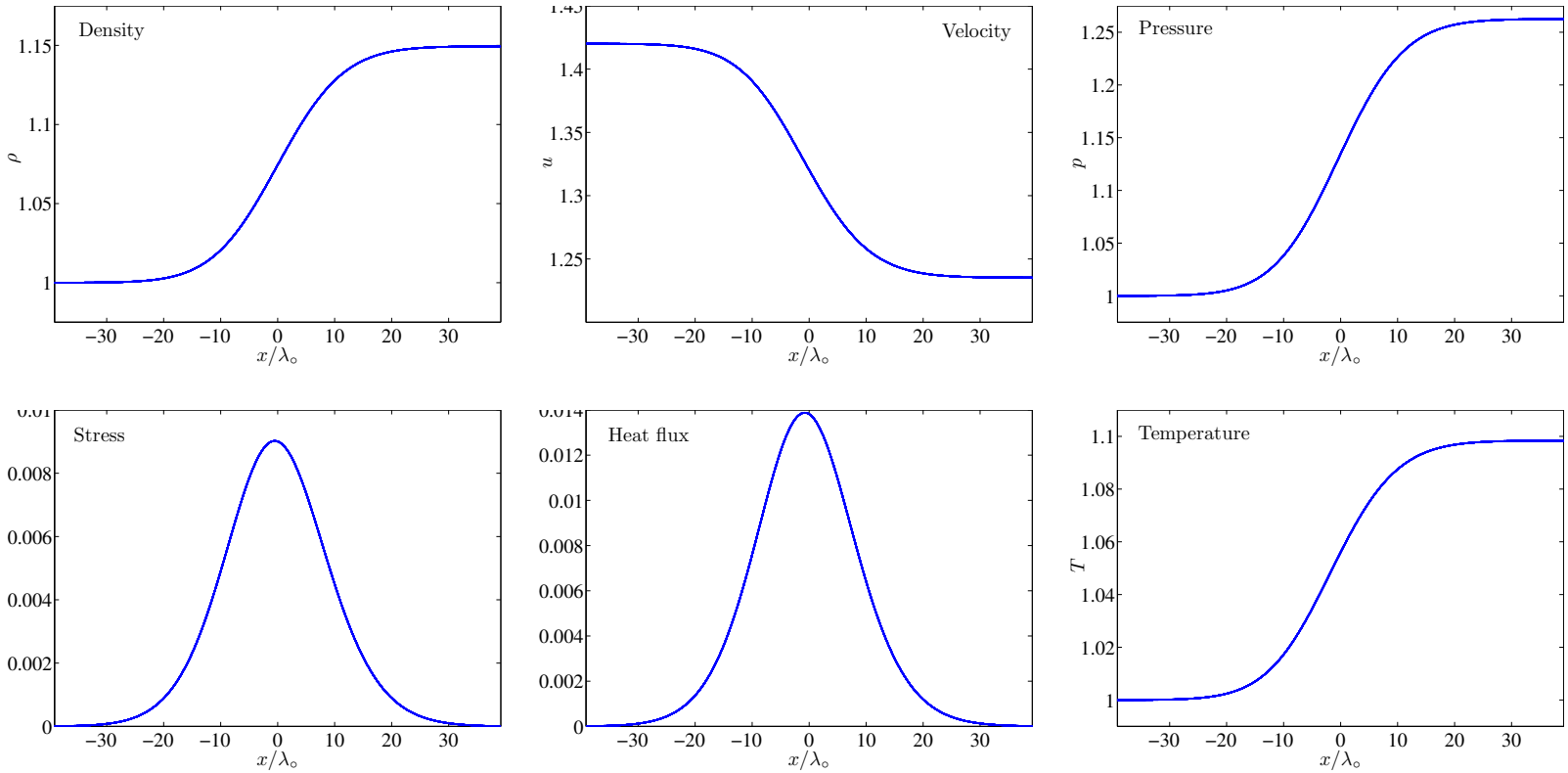


Figure: G13 (—) solution obtained for a Mach 1.1 shock with $\Delta x \approx 0.04\lambda_\circ$. The indicated profiles are smooth since the shock speed is lower than that of the maximum eigenvalue, with the R13 solution being nearly identical to the G13 solution.

Mach 1.651 Shock with 13 Moment Equations

Third-order finite volume solution using Roe's flux-difference splitting

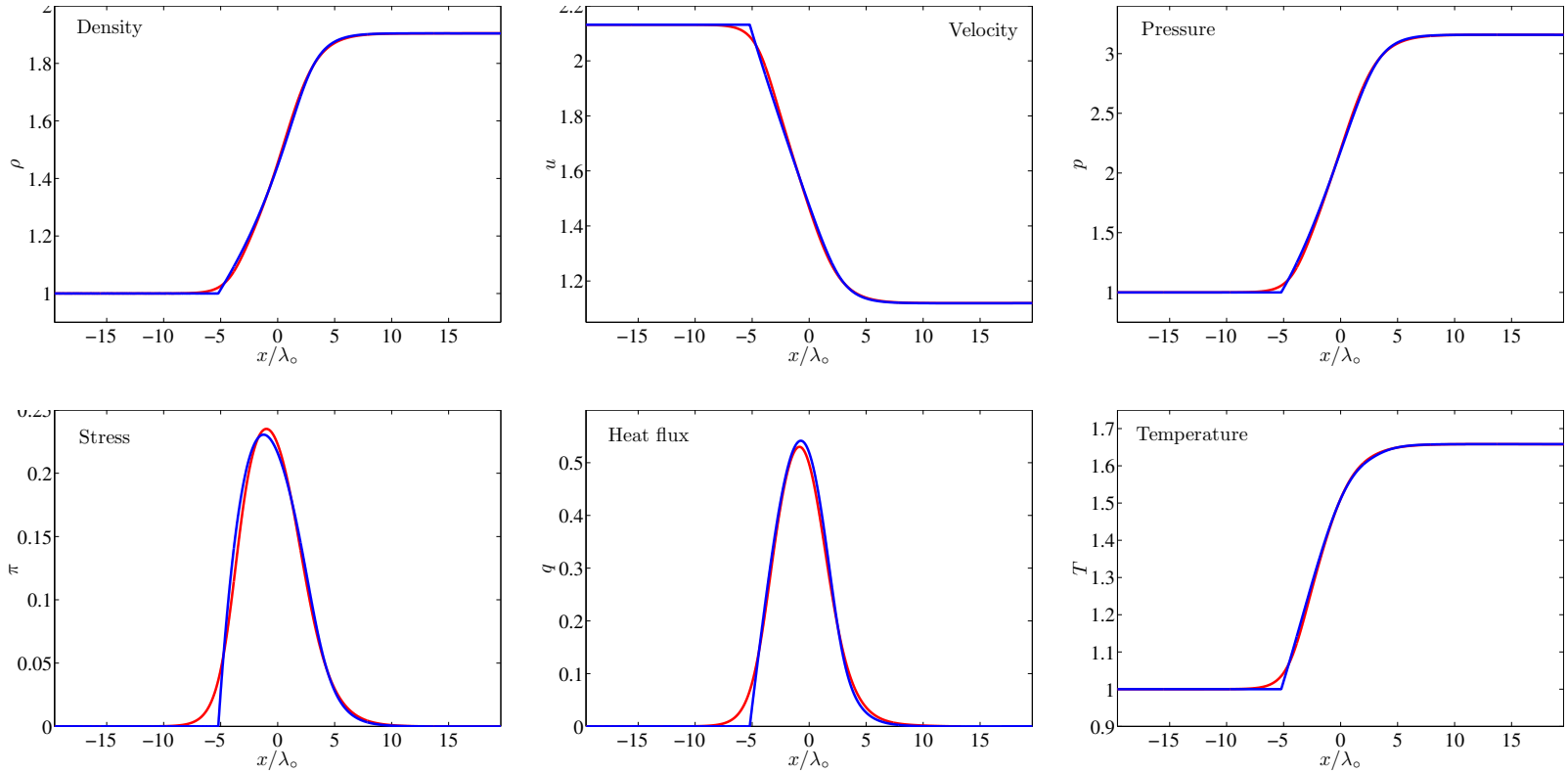


Figure: G13 (—) and R13 (—) solutions obtained for a Mach 1.651 shock with $\Delta x \approx 0.02\lambda_\circ$. As the free-stream shock speed approaches the maximum characteristic wave speed, a discontinuity begins to develop at the onset of the shock.

Mach 6.0 Shock with 13 Moment Equations

First-order finite volume solution using Roe's flux-difference splitting

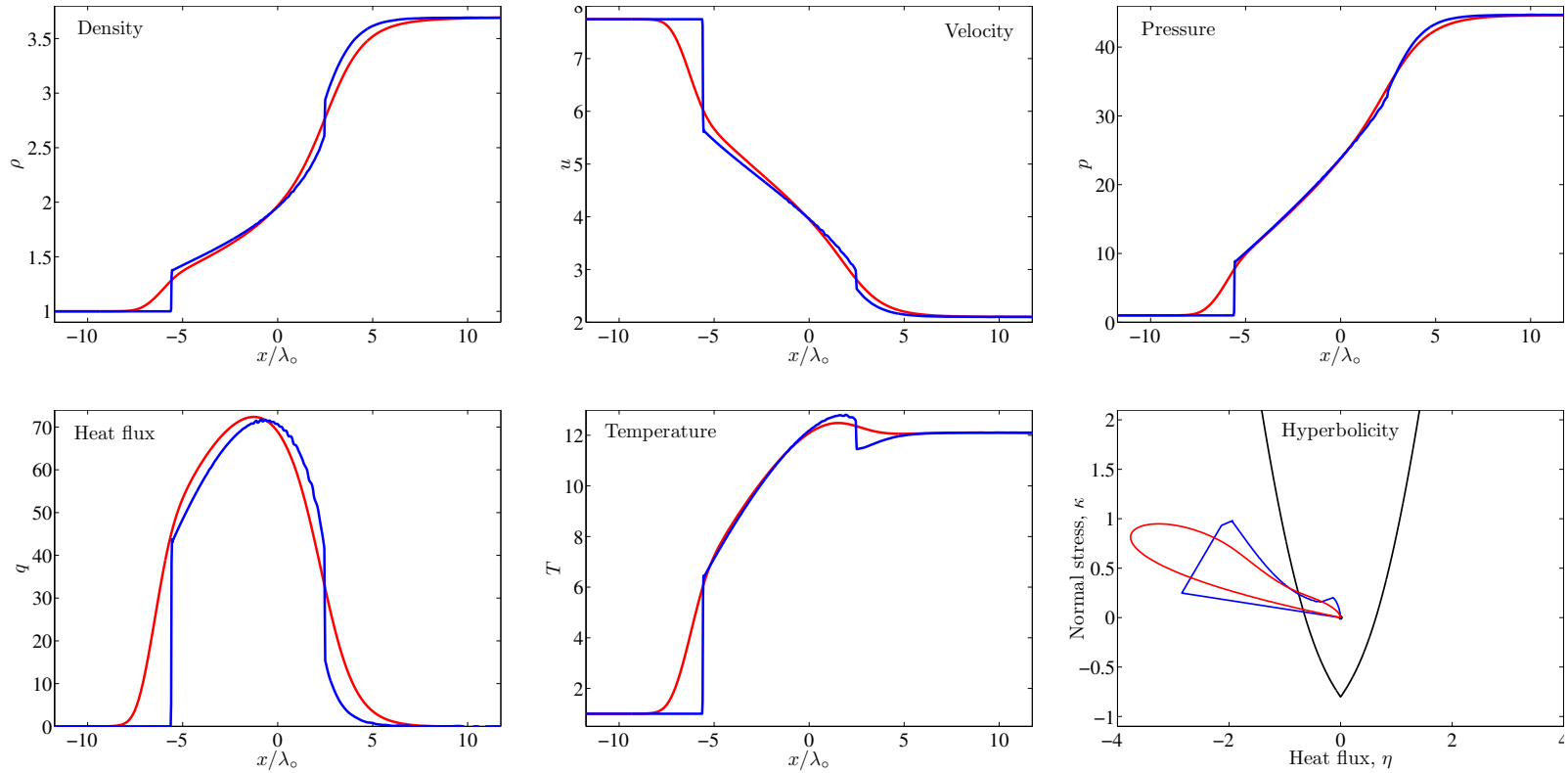
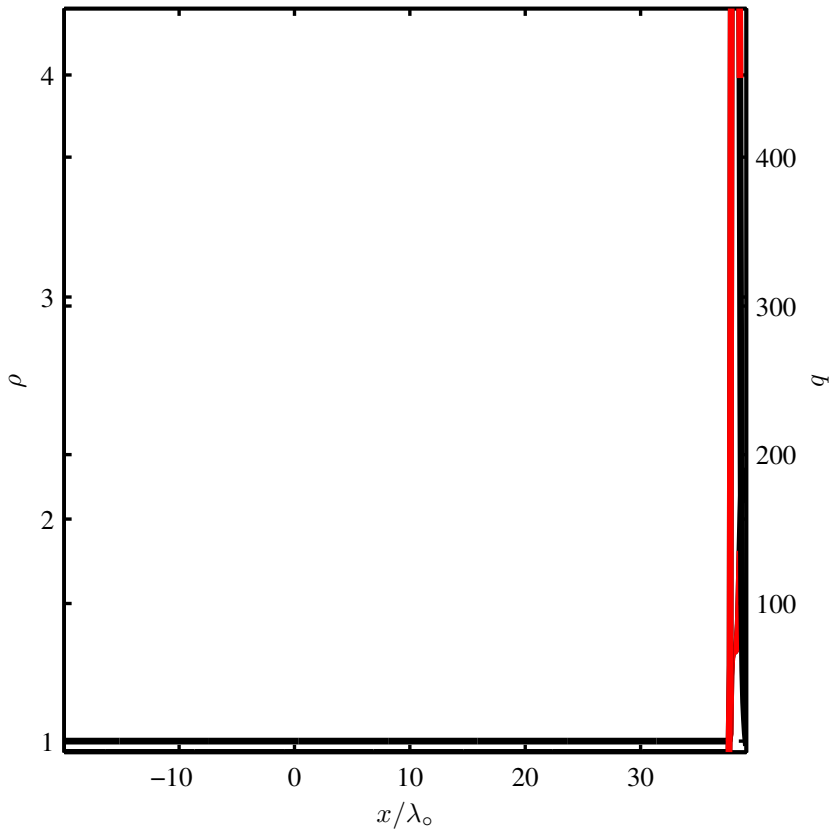


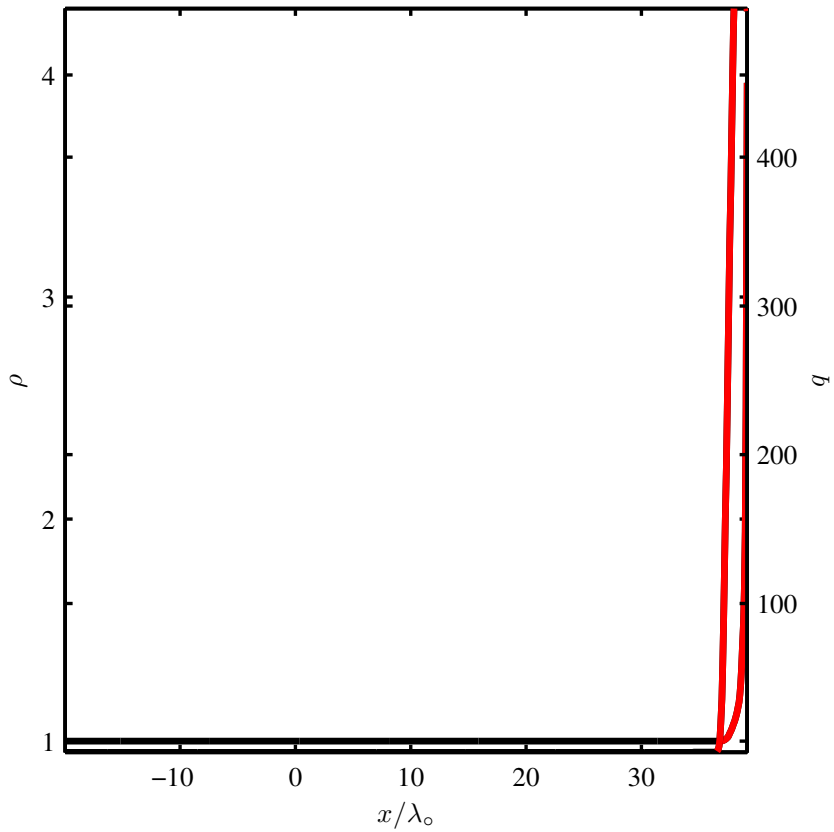
Figure: G13 (—) and R13 (—) solutions obtained for a Mach 6.0 shock with $\Delta x \approx 0.02\lambda_\circ$. Beyond $\mathrm{Ma}_\circ \approx 3.5$, a second subshock develops in the G13 solution at the inflection point. For this case, the subshock is already quite pronounced. Both subshocks are smoothed away by regularization terms.

Mach 10 Shock with 13 Moment Equations

- Grad 13 (1958)



- Regularized 13 (2003)



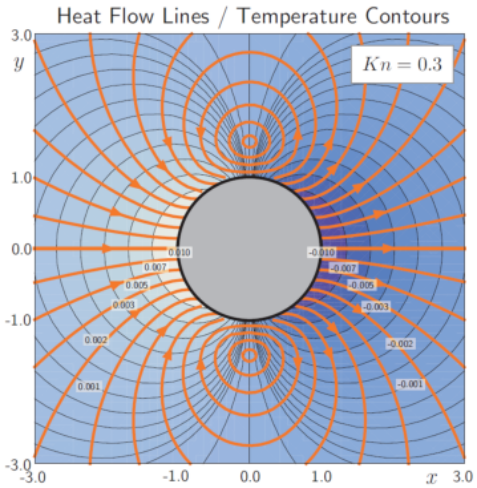
R13 Examples

Much effort has been made to develop moment methods which has met with great success in obtaining stable solutions for aerospace applications, including shock wave structures (Torillhon & Struchtrup, 2004)

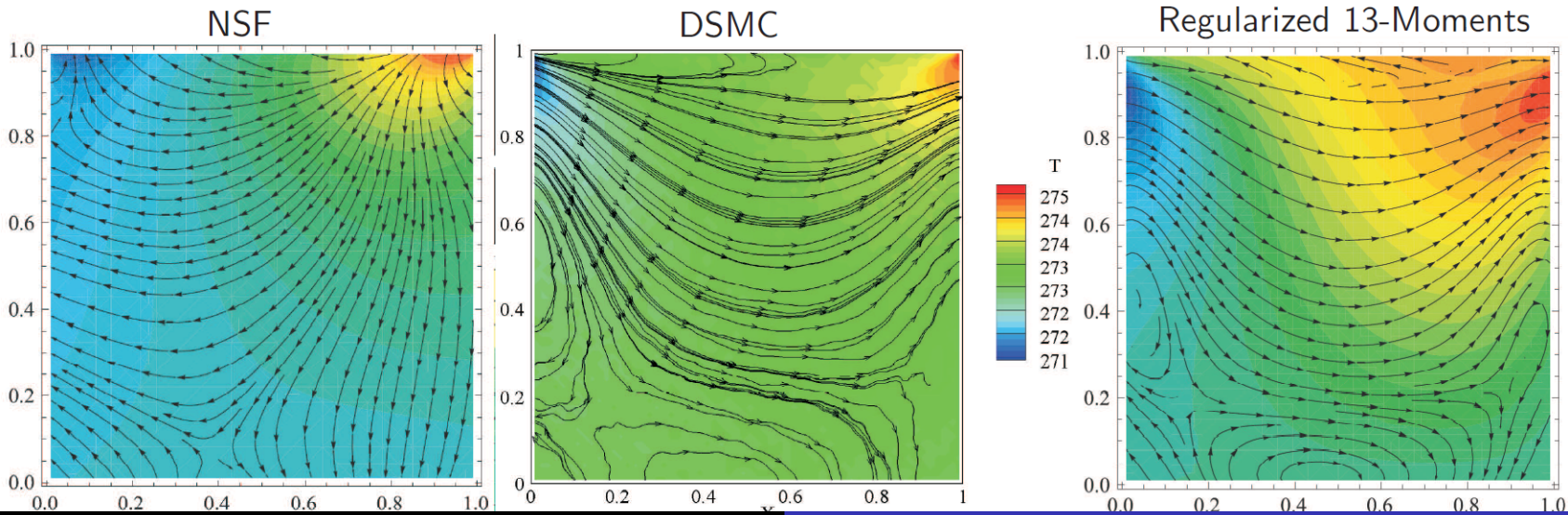
13-moment equations can :

- obtain solutions when Navier-Stokes fails as in the case of driven cavity flow
- predict counter-intuitive coupling of fields, resulting in exotic behavior

R13 sphere (Torrilhon 2010)



Driven cavity flow (Rana et al. 2010)



Outline

1. Governing equations
2. Numerical Formulation
3. Benchmarks
4. Collisional-Radiative Model
5. UTIAS Shocktube Experiments
6. Extensions & ongoing research
7. Moment equations
8. Conclusions

Conclusions and Acknowledgments

- A highly-accurate Collisional-Radiative model for argon has been developed and coupled with a high-order, time-accurate shock-capturing scheme
- The Collisional-Radiative model makes use of the latest cross sections and Object-Oriented programming
- First time that the dynamic structure of a multi-dimensional ionizing shock has been simulated
- Progress is being made in extending the models to other nonequilibrium aspects

- We wish to acknowledge the support of:
  - EOARD grant No. FA8655-10-1-3076 (PM: Dr. G. Abate)
  - AFOSR, grant No. 02PR05COR (PM: Dr. F. Fahroo)
  - European Research Council grant

Thank you for your attention!

